

AEDC-TR-66-181

copy

**ARCHIVE COPY
DO NOT LOAN**



**CONSTANT ACCELERATION FLOWS AND
APPLICATIONS TO HIGH-SPEED GUNS**

J. Lukasiewicz

ARO, Inc.

November 1966

Distribution of this document is unlimited.

**VON KÁRMÁN GAS DYNAMICS FACILITY
ARNOLD ENGINEERING DEVELOPMENT CENTER
AIR FORCE SYSTEMS COMMAND
ARNOLD AIR FORCE STATION, TENNESSEE**

PROPERTY OF U. S. AIR FORCE
AEDC LIBRARY
AF 40(600)1200

AEDC TECHNICAL LIBRARY



LT9E TE000 0220 5

NOTICES

When U. S. Government drawings, specifications, or other data are used for any purpose other than a definitely related Government procurement operation, the Government thereby incurs no responsibility nor any obligation whatsoever, and the fact that the Government may have formulated, furnished, or in any way supplied the said drawings, specifications, or other data, is not to be regarded by implication or otherwise, or in any manner licensing the holder or any other person or corporation, or conveying any rights or permission to manufacture, use, or sell any patented invention that may in any way be related thereto.

Qualified users may obtain copies of this report from the Defense Documentation Center.

References to named commercial products in this report are not to be considered in any sense as an endorsement of the product by the United States Air Force or the Government.

CONSTANT ACCELERATION FLOWS AND
APPLICATIONS TO HIGH-SPEED GUNS

J. Lukasiewicz
ARO, Inc.

Distribution of this document is unlimited.

FOREWORD

The research reported herein was sponsored by the Arnold Engineering Development Center (AEDC), Air Force Systems Command (AFSC), Arnold Air Force Station, Tennessee, under Program Element 65402234. The work was done by ARO, Inc. (a subsidiary of Sverdrup & Parcel and Associates, Inc.), contract operator of AEDC, AFSC, under ARO Project No. VG2706, and the manuscript was submitted for publication on August 26, 1966.

The help given by Messrs. W. C. Armstrong and C. T. Bell, ARO, Inc., who have programmed the numerical solutions for ideal and real hydrogen, and by Messrs. A. J. Cable and J. R. DeWitt, ARO, Inc., who have supplied the experimental and computed base pressure histories, is gratefully acknowledged by the author.

This technical report has been reviewed and is approved.

Donald E. Beitsch
Major, USAF
AF Representative, VKF
Directorate of Test

Leonard T. Glaser
Colonel, USAF
Director of Test

ABSTRACT

Solutions for isothermal, isentropic, and constant Mach number (at a specified location) flows with constant acceleration are obtained. It is shown that in application to high-speed guns, these solutions necessitate variable gun geometry or heating of the propellant; both requirements are considered at present impractical. Numerical solutions which give constant projectile acceleration in a fixed geometry gun are computed for ideal and real hydrogen propellant. Using the latter, and the appropriate similarity parameters, as well as practical constraints related to gun and projectile geometry and strength, it is shown that a substantial increase in muzzle velocity could be obtained if the constant base pressure cycle were more closely approximated in actual launchings. At present the velocity attained with large caliber guns is much smaller than with the small ones. In this connection, the validity of linear scaling of guns and the resulting possibility of application of small-scale developments to large caliber guns are indicated.

CONTENTS

	<u>Page</u>
ABSTRACT	iii
NOMENCLATURE	vi
I. INTRODUCTION	1
II. CONSTANT ACCELERATION FLOWS	
2.1 Isothermal Flow	2
2.2 Isentropic Flow	3
2.3 Flow with Constant Mach Number at a Specified Location	5
III. APPLICATIONS TO IDEAL LAUNCH CYCLES	
3.1 Homogeneous Constant Acceleration Solutions	7
3.2 Nonhomogeneous, Constant Acceleration Solutions	9
IV. GUN PERFORMANCE AND SCALING	
4.1 Limitations of Gun Performance	12
4.2 Linear Scaling of Guns	15
V. CONCLUSIONS	17
VI. REFERENCES	18

ILLUSTRATIONS

Figure

1. Pressure and Density Distribution in Isothermal Flow (Isothermal Atmosphere, $\gamma = 1.4$)	19
2. Isothermal Flow	20
3. Pressure Distribution in Isentropic Flow ($\gamma = 1.4$)	21
4. Isentropic Flow ($\gamma = 1.4$)	22
5. Distribution of Parameters of State for Flow with $M_0 = 1$ ($\gamma = 1.4$)	23
6. Flow with $M_0 = 1$ ($\gamma = 1.4$)	24
7. Typical Gun Configuration (Final Stage of a Light-Gas Gun)	25
8. Variation of Pump Tube Pressure with Time	26
9. Variation of Pump Tube Temperature with Time	27
10. Variation of Pump Tube Pressure with Characteristic Time τ''	28
11. Variation of Pump Tube Temperature with Characteristic Time τ''	29

<u>Figure</u>	<u>Page</u>
12. Nonhomogeneous Solution for Constant Geometry and Acceleration, Isentropic Launch Cycle	30
13. Characteristic Solution of Nonhomogeneous, Isentropic Flow ($\gamma = 1.4$)	31
14. Rates of Mass Flow for Homogeneous and Nonhomogeneous, Isentropic Solutions	32
15. Characteristic Solution of Nonhomogeneous Flow of Real Hydrogen	33
16. Performance of Guns and Materials	34
17. Maximum Launch Velocities and Weights	35
18. Measured and Computed Base Pressure in a 0.5-in. -caliber Gun (Low Base Pressure Peak)	36
19. Measured and Computed Base Pressure in a 0.5-in. -caliber Gun (High Base Pressure Peak),	37
20. Computed Base Pressures for Linearly Scaled Guns	38

TABLES

I. Isentropic Flow, $\gamma = 1.4$	39
II. Hydrogen Thermodynamic Data for $s/R = 16$, $T = 100(100) 3900^\circ\text{K}$ (Ref. 5)	40
III. Hydrogen Data for Characteristic Computations.	41
IV. Isentropic Flow, Real Hydrogen.	42
V. Deviations from Exact Linear Scaling as Used in Launch Cycle Calculations and Actual Shots	43

NOMENCLATURE

A	Cross-sectional area
a	Velocity of sound
$C_{+,-}$	Eq. (3)

d	Diameter, caliber
F	Eq. (3)
\bar{F}	F/a_0
g	Gravitational acceleration
k	Eq. (26)
l_g	Projectile length
l_o	Barrel length
l_p	Piston length
l_{pt}	Pump tube length
M	Mach number
m	Mass per unit area
m_∞	Eq. (4)
p	Pressure
Q	Heat per unit mass
R	Gas constant
T	Temperature
t	Time
t_o, \bar{t}_o	At $x = \bar{x} = 0$
\bar{t}''	Fig. 4
\bar{t}'	Fig. 12
u	Velocity
x	Length
x_o, \bar{x}_o	At $t = \bar{t} = 0$
a	Acceleration
β	l_o/d
Γ	Eq. (10)
γ	Ratio of specific heats
δ	Eq. (28)
ϵ	l_1/d
λ	Eq. (25)

ρ	Gas density
ρ_l	Projectile density
ρ_p	Piston density
ω	Eq. (27)
$()_o$	Reference conditions or projectile base conditions
$()_p$	Pump tube (reservoir) conditions
$()^*$	Sonic conditions
$\bar{()}, \hat{()}$	Dimensionless variables defined in text

SECTION I INTRODUCTION

Simple models of the earth's atmosphere, for which a constant gravitational field was assumed (Ref. 1), provide early examples of one-dimensional situations of gases subjected to a constant acceleration. More recently, this type of flow was considered by Stanyukovitch (Ref. 2), and the interest was renewed (Ref. 3) in connection with the design and optimization of high velocity, two-stage, light-gas launchers. In this report various types of constant acceleration flows are considered, and the results are applied to calculate the idealized performance of the final stage of a constant base pressure launcher, using either perfect gas ($\gamma = 1.4$) or real hydrogen propellant. In the light of these results, limitations and scaling of high-speed guns are discussed.

SECTION II CONSTANT ACCELERATION FLOWS*

The analysis of constant acceleration flows of various types is based on the following relations:

- (i) The motion resulting from uniform acceleration is given, in the Eulerian coordinate x , by

$$x = x_0 + at^2/2 \quad (1)$$

with

$$u = at \text{ and } x = x_0 \text{ at } t = 0;$$

- (ii) From Newton's Second Law, for flows characterized by a constant acceleration a and in the absence of forces other than fluid pressure (e. g., body forces and frictional forces), the pressure distribution is given in the Lagrangian coordinate x_0 by

$$-dp/dx_0 = a\rho \quad (2)$$

For example, Eq. (2), with $x_0 = \text{height}$, gives the pressure gradient for an atmosphere in a constant gravitational field a ;

- (iii) A pressure-density relationship necessary for the solution of Eq. (1) is postulated according to the desired type of the thermodynamic process in the gas, e. g., isothermal, isentropic, or other stipulated condition, e. g., constancy of Mach number at a specified location;

*Unless otherwise stated, all numerical values and plots given in this report are for $\gamma = 1.4$.

- (iv) An equation of state ($p/\rho = gRT$, is used here), or numerical real gas thermodynamic data provide the necessary relationships between other thermodynamic parameters;
- (v) In order to interpret some of the results, and to compute more complex flow fields, the method of characteristics is used. Equations of characteristics in one-dimensional, unsteady flow (Ref. 4), are written

$$F \pm u = C_{+,-} \tag{3}$$

with

$$F = \int dp/(\rho a)$$

and the signs corresponding to the slopes

$$dx/dt = u \pm a$$

It is evident from Eq. (2) that, in the Lagrangian coordinate, constant acceleration flows are steady; in the Eulerian frame of reference such flows are quasi-steady, the velocity being dependent on time alone.

In view of the constancy of acceleration, the pressure p at station x_0 is a direct measure of the total mass per unit area of the accelerated medium m_∞ ahead of station x_0 (or of the mass per unit area of an atmosphere above height x_0). Thus, from Eq. (2),

$$m_\infty = \int_{x_0}^{\infty} \rho dx_0 = p/a \tag{4}$$

It is convenient to introduce at this point dimensionless variables as follows:

$$\bar{x} = ax/a_0^2, \bar{t} = at/a_0, \bar{u} = u/a_0 = \bar{t}, \bar{a} = a/a_0$$

$$\bar{p} = p/p_0, \bar{\rho} = \rho/\rho_0$$

where $()_0$ refers to the state at $x = 0, t = 0$.

The dimensionless equation of motion then reads

$$\bar{x} - \bar{x}_0 = \frac{1}{2} \bar{t}^2 \tag{5}$$

2.1 ISOTHERMAL FLOW

For the case of isothermal, perfect gas flow $a_0 = \text{constant}$ and Eq. (2) reads

$$\bar{x}_0 = (-1/\gamma) \ln \bar{p} \tag{6}$$

The Mach number is given by $M = u/a_0 = \bar{v}$.

Equation (6) and Fig. 1 give density and pressure distributions in an isothermal atmosphere in a gravitational field a (Ref. 1), or in isothermal flow with constant acceleration. The length $(1/\gamma)$, Fig. 1, subtended by the pressure gradient at $\bar{x}_0 = 0$ is the height which the atmosphere would have if it were of constant density $\bar{\rho} = 1$.

The characteristic equations are

$$(1/\gamma) \ln \bar{p} \pm \bar{u} = C_{+,-} \quad (7)$$

and hence

$$\bar{x} - \bar{x}_0 = \frac{1}{2} \bar{v}^2 \pm \bar{v}$$

In Fig. 2, isothermal flow is illustrated in the \bar{x} , \bar{v} coordinates, with the pathline $\bar{p} = \bar{\rho} = 1$ and characteristics passing through $\bar{x} = 0$, $\bar{v} = M = 1$ being shown.

2.2 ISENTROPIC FLOW

For isentropic flow of a perfect gas, $p\rho^{-\gamma} = \text{constant}$, Eq. (2) gives

$$\bar{x}_0 = -(\bar{p}^{(\gamma-1)/\gamma} - 1)/(\gamma-1) \quad (8)$$

The pressure vanishes at $\bar{x}_0 = 1/(\gamma-1)$. The distribution of pressure is shown in Fig. 3.

The various features of isentropic flow, as discussed below, are indicated in Fig. 4 in the \bar{x} , \bar{v} plane.

The Mach number is given, from Eqs. (5) and (8) by

$$1 - (\gamma-1)\bar{x} + [(\gamma-1)/2 - 1/M^2]\bar{v}^2 = 0 \quad (9)$$

For all values of M , $\bar{x}_0 = 1/(\gamma-1)$; also, at this value of \bar{x} the Mach number remains constant at $[2/(\gamma-1)]^{1/2} = \sqrt{5}$. At $\bar{x} = \frac{1}{2}\bar{v}^2 + 1/(\gamma-1)$, the Mach number becomes infinite while the pressure, density, and temperature vanish. Along the pathline $\bar{p} = 1$, the Mach number distribution is $M = \bar{u} = \bar{v} = \sqrt{2\bar{x}}$.

At station $\bar{x} = 0$, the variation of state parameters is given by

$$\bar{p} = \Gamma^{\gamma/(\gamma-1)}, \bar{\rho} = \Gamma^{1/(\gamma-1)}, \bar{T} = \bar{a}^2 = \Gamma, M = \Gamma^{-1/2}\bar{v} \quad (10)$$

with $\Gamma = 1 + (\gamma-1)\bar{v}^2/2$.

Of particular interest are sonic ($M = 1$) conditions denoted by $*$. From Eq. (9),

$$1 - (\gamma - 1) \bar{x}^* - (3 - \gamma) \bar{t}^{*2} / 2 = 0 \quad (11)$$

giving

$$\bar{t}_o^* = \bar{u}^* = \bar{a}^* = \sqrt{\bar{T}^*} = \sqrt{2/(3 - \gamma)} = 1.118$$

$$\bar{T}^* = 1.25$$

$$\bar{\rho}^* = \bar{T}^{*1/(\gamma - 1)} = 1.746$$

$$\bar{p}^* = \bar{\rho}^* \gamma = 2.184$$

In isentropic, unsteady flow the characteristics are given by

$$\bar{u} \pm [2/(\gamma - 1)] \bar{a} = C_{+,-} \quad (12)$$

and hence

$$\bar{t} \pm [2/(\gamma - 1)] [1 + (\gamma - 1)/(\bar{t}^2/2 - \bar{x})]^{1/2} = C_{+,-}$$

For characteristics through \bar{t}_o^* ,

$$C_+ = \frac{\gamma + 1}{\gamma - 1} \sqrt{\frac{2}{3 - \gamma}} = 6.708$$

$$C_- = -\sqrt{2(3 - \gamma)/(\gamma - 1)} = -4.472$$

The C_+ characteristic which passes through \bar{t}_o^* intercepts the $\bar{p} = 1$ pathline at

$$\bar{t}'' = M'' = \bar{u}'' = [(\gamma + 1) \sqrt{2/(3 - \gamma)} - 2]/(\gamma - 1) = 1.708 \quad (13)$$

$$\bar{x}'' = \bar{t}''^2/2 = 1.459$$

In general, the relationship between the \bar{t}'' at which a C_+ characteristic intercepts the $\bar{p} = 1$ pathline, and the time \bar{t}_o'' at which the same characteristic intercepts the $\bar{x} = 0$ coordinate, is given from Eqs. (5) and (12):

$$\bar{t}'' = \bar{t}_o'' + \frac{2}{\gamma - 1} \left\{ [1 + (\gamma - 1) \bar{t}_o''^2/2]^{1/2} - 1 \right\} \quad (14)$$

2.3 FLOW WITH CONSTANT MACH NUMBER AT A SPECIFIED LOCATION

Consider a flow with constant acceleration in which a constant Mach number M_0 is maintained at $x = 0$. For such a flow

$$u_{x=0,t} = M_0 a_{x=0,t} = at_0 \quad (15)$$

and, using Eq. (1), the distribution of velocity of sound (and temperature) at time $t = 0$ is given by

$$x_0 = - M_0^2 a^2 / 2a = - \gamma R T M_0^2 / (2a) \quad (16)$$

Thus the flow of the type considered here exhibits a linear temperature distribution in x_0 . The equation of motion (Eq. (1)) becomes

$$x + a^2 M_0^2 / (2a) = at^2 / 2 \quad (17)$$

From Eqs. (2) and (16), the parameters of state are related by

$$pa^{-\gamma M_0^2} = \text{constant}$$

The equations of the characteristics are written

$$M_0^2 a \pm u = C_{+, -} \quad (18)$$

It is apparent from Eq. (16) that the Mach number is indeterminate at $x = 0$, $t = 0$ (with $u = T = 0$), and therefore it is convenient in this case to normalize the equations with respect to conditions at $x = 0$, $t = t_0^1$. Putting

$$\hat{x} = ax/a_{t_0}^2, \hat{t} = at/a_{t_0}, \hat{a} = a/a_{t_0}, \hat{\rho} = \rho/\rho_{t_0}$$

$$\hat{u} = u/a_{t_0} = \hat{t}, \hat{p} = p/p_{t_0}, \hat{T} = T/T_{t_0}$$

the properties of the flow are related by

$$\hat{T} = \hat{a}^2 = \hat{p} \frac{2}{\gamma M_0^2} = \rho \frac{2}{\gamma M_0^2 - 2} = -2\hat{x}_0/M_0^2 = (\hat{t}_0/M_0)^2 \quad (19)$$

The entropy distribution relative to the reference state, $\Delta s = s - s_{t_0}^1$, is given by

$$\Delta \hat{s} = \Delta s/R = [\gamma/(\gamma-1)] \ln \hat{T} - \ln \hat{p} = \gamma [1/(\gamma-1) - M_0^2/2] \ln \hat{T} \quad (20)$$

The above distributions of parameters of state are plotted for $M_0 = 1$ in Fig. 5.

The equation of motion is written

$$2\hat{x} + M_0^2 \hat{a}^2 = \hat{t}^2 \quad (21)$$

and, since $M = \bar{t}/\bar{a}$, the constant Mach number lines are given by

$$\hat{x} = [1 - (M_0/M)^2] \hat{t}^2/2 \quad (22)$$

Using Eq. (21), the characteristic equations are

$$M_0 \sqrt{\hat{t}^2 - 2\hat{x}} \pm \hat{t} = C_{+,-} \quad (23)$$

The relationship between the time \hat{t}'' at which a C_+ characteristic intercepts the $\hat{p} = 1$ pathline, and the time \hat{t}_0'' at which the same characteristic intercepts the $\hat{x} = 0$ coordinate is given, from Eqs. (21) and (23) by

$$\hat{t}'' + M_0 = \hat{t}_0'' (1 + M_0) \quad (24)$$

For the particular case of $M_0 = 1$, the flow is shown in the \hat{x}, \hat{t} plane in Fig. 6. In addition to pathlines and $M = \text{constant}$ lines, the characteristics through $(\hat{x} = 0, \hat{t} = 2)$ are drawn; the C_- characteristic coincides with the \hat{t} coordinate.

SECTION III APPLICATIONS TO IDEAL LAUNCH CYCLES

Consider a typical configuration of the final stage of a light-gas gun, shown in Fig. 7. A light-gas propellant, while being compressed in the pump tube by a piston, expands into the barrel and accelerates the projectile. If it were assumed that the projectile could withstand some maximum acceleration irrespective of the duration of its application (i. e., neglecting the dynamic effects of projectile loading), then for a given projectile and a given barrel length the maximum muzzle velocity would be obtained by continuous application of such acceleration. Based on this consideration the so-called constant projectile base pressure cycle has often been considered (e. g., Ref. 3) as the one most desirable for use in high velocity guns.

The applicability of the previously derived, homogeneous, constant acceleration flow solutions (in which all of the propellant maintains constant acceleration), and other, nonhomogeneous solutions (in which only part of the propellant adjacent to the projectile moves with constant acceleration) to the constant base pressure gun cycle will be examined in the following sections.

3.1 HOMOGENEOUS, CONSTANT ACCELERATION SOLUTIONS

Suppose the propellant flow to be isentropic, the projectile to be initially located at $\bar{x} = 0$ and a constant pressure $\bar{p} = 1$ to be maintained at its base. A constant acceleration solution for flow in the barrel would satisfy these requirements, with the conditions at the barrel entrance ($\bar{x} = 0$) being matched on the basis of isentropic expansion across the pump tube/barrel area change. The propellant in the pump tube can be considered to be virtually at rest*, the pump tube conditions corresponding at all times to the isentropic reservoir conditions (denoted by subscript p), and the required piston motion being thus determined. The time variations of pump tube (reservoir) pressure and temperature are given in Table I and in Figs. 8 and 9, curves "a". Figures 10 and 11 show the pressure \bar{p}_p and temperature \bar{T}_p required to attain projectile velocity $\bar{u} = \bar{\tau}''$, where $\bar{\tau}''$ is related to $\bar{\tau}_o$ by a C_+ characteristic, cf. Eq. (14) and Fig. 4.

Since in this type of flow the Mach number at the barrel entrance ($\bar{x} = 0$) attains supersonic values for times in excess of $\bar{\tau}_o^* = \sqrt{2/(3-\gamma)}$, Eq. (11), a variable-geometry barrel entrance (e. g., vented entrance or variable area throat) would be required to maintain constant acceleration flow beyond a velocity $\bar{u}'' = 1.708$, Eq. (13). The maximum required area contraction (at $\bar{\tau} \rightarrow \infty$) would be

$$A^*/A = \left(\frac{\gamma+1}{4}\right)^{\frac{\gamma+1}{2(\gamma-1)}} \left(\frac{2}{\gamma-1}\right)^{\frac{1}{2}} = 0.483$$

It is possible to envisage mechanical schemes with which the above variable-geometry requirements could be satisfied. However, in view of the extreme pressures and temperatures which occur in practice in the region of pump tube/launch tube juncture, such solutions must be at present considered academic, at least as regards attainment of maximum projectile velocities.

It was shown that in isentropic, constant acceleration flow a constant Mach number is maintained at the station $\bar{x} = 1/(\gamma-1)$, Eq. (9). This could imply a constant barrel entrance area expansion giving the required Mach number, but would necessitate the projectile to enter the barrel with a velocity $\bar{u} = [2/(\gamma-1)]^{\frac{1}{2}}$. Again, mechanical means required to accomplish this appear impractical.

*For, say, a pump tube/barrel diameter ratio of 3 or 4, this is an excellent approximation for all launch tube entry Mach numbers.

Since in a practical, constant-geometry gun the flow must become choked at the barrel entrance, the applicability of the nonisentropic, constant Mach number solution at $\bar{x} = 0$ is of interest. The required launch cycle can be envisaged as consisting of two phases: first, an isentropic phase, during which propellant attains sonic velocity at the barrel entrance, and, secondly, a nonisentropic phase, during which constant acceleration is maintained while the flow remains sonic at the barrel entrance.

The variation of the propellant state at the barrel entrance is given, during the first phase, by Eq. (10), and during the second phase by Eq. (19). The reference conditions $a_{t_0}^*$, $p_{t_0}^*$, etc., have to be identified with the isentropic, sonic flow conditions, Eq. (11). Accordingly, Eq. (19) gives, for $\bar{\tau} \geq [2/(3 - \gamma)]^{1/2} = 1.118$,

$$\begin{aligned} \bar{p} &= \lambda \bar{\tau}^\gamma, \quad \bar{\rho} = \lambda \bar{\tau}^{(\gamma-2)}, \quad \bar{T} = \bar{\tau}^2 \\ \bar{\rho} \bar{u} &= \lambda \bar{\tau}^{(\gamma-1)} \end{aligned} \tag{25}$$

with

$$\lambda = [2/(3 - \gamma)]^{\frac{\gamma(3-\gamma)}{2(\gamma-1)}} = 1.868$$

The corresponding pump tube or reservoir propellant state, denoted by subscript p , is given (at $\bar{\tau} \geq \bar{\tau}_0^*$) under the assumptions of negligible flow velocity in the pump tube and isentropic acceleration to the sonic velocity at the barrel entrance, by Eq. (25) multiplied by the isentropic sonic ratios as follows:

$$\begin{aligned} \bar{p}_p &= k \frac{\gamma}{\gamma-1} \bar{p} = 1.893 \bar{p} \\ \bar{\rho}_p &= k \frac{\gamma}{\gamma-1} \bar{\rho} = 1.577 \bar{\rho} \\ \bar{T}_p &= k \bar{T} = 1.2 \bar{T} \end{aligned} \tag{26}$$

with

$$k = (\gamma + 1) / 2 = 1.2$$

The pump tube pressure and temperature are given in terms of time $\bar{\tau}_0$ in Table I and Figs. 8 and 9, curves "b".

In order to determine the time at which the projectile is affected by the conditions at the barrel entrance, it is necessary to consider

the C_+ characteristic which passes through the two phases of flow (for $\bar{t} > \bar{t}_0^*$). In terms of dimensionless variables appropriate to the isentropic flow case, the times \bar{t}'' and \bar{t}_0'' at which a C_+ characteristic intercepts the projectile path ($\bar{p} = 1$) and the barrel entrance ($\bar{x} = 0$), respectively, are given by

$$\bar{t}'' = 2\bar{t}_0'' + \omega \quad (27)$$

where

$$\omega = \sqrt{2} (\sqrt{3 - \gamma} - \sqrt{2}) / (\gamma - 1) = -0.528$$

The pump tube pressure and temperature are plotted in terms of $\bar{u} = \bar{t}''$ in Figs. 10 and 11, curves "b". It is apparent that, compared with the isentropic case, this solution results in much higher temperatures and lower pressures in the pump tube.

In the cycle here considered, the second phase involves heating of the propellant. The amount of heat required per unit mass of propellant is given by, Eq. (20),

$$\bar{Q} = \int T ds / (R T_0) = \delta (\bar{T} - \frac{2}{3 - \gamma}) \quad (28)$$

with

$$\delta = \gamma [1/(\gamma - 1) - 1/2] = 2.8$$

and, from Eq. (25), the rate of heat flow per unit barrel cross-sectional area is

$$\begin{aligned} \bar{Q} \bar{\rho} \bar{u} &= \delta \lambda [\bar{T}^2 - 2/(3 - \gamma)] \bar{T}^{(\gamma-1)} \\ &= 5.23 (\bar{T}^2 - 1.25) \bar{T}^{0.4} \end{aligned} \quad (29)$$

This is the ideal rate at which the pump tube gas would have to be heated just upstream of the barrel entrance to insure constant acceleration propellant flow in a fixed-geometry gun.

3.2 NONHOMOGENEOUS, CONSTANT ACCELERATION SOLUTIONS

If the insistence on the homogeneity of the motion in the launch tube were relaxed, other solutions applicable to the constant base pressure gun cycle would be possible. The one of particular interest is the isentropic solution suggested by Smith (Ref. 3), who presented some results in graphical form. Here solutions of this type are considered in some detail, including numerical results of computations for an ideal ($\gamma = 1.4$) and for real hydrogen propellant.

As has been shown, the difficulty in maintaining a constant acceleration, isentropic flow arises in a constant-geometry launcher after

time \bar{t}_0^* , at which sonic conditions are first attained at the barrel entrance. Unless a variable throat can be formed at the entrance, choking will prevent maintenance of a constant acceleration flow. However, an isentropic flow solution can be obtained in which sonic flow at the barrel entrance and constant acceleration in the part of the flow field adjacent to the projectile are maintained.

Consider constant acceleration, isentropic flow in the \bar{x}, \bar{t} plane, Fig. 12. From the theory of characteristics (Ref. 4) it follows that the region in which the flow is uniquely determined is bounded by a segment of the \bar{x}, \bar{t} path (projectile path in this case) and by two intersecting characteristics originating at the extremities of the path. Therefore, in order to maintain constant acceleration up to time \bar{t}'' , it is sufficient to match the solution along characteristic C_-^* until time \bar{t}' . The matching flow solution can be computed, since conditions along characteristic C_-^* are given, the flow is isentropic and the requirement of sonic flow at $\bar{x} = 0$ has to be satisfied.

3.2.1 Ideal Propellant ($\gamma = 1.4$)

The solution has been programmed using $\Delta \bar{t} = 0.005$ intervals along the C_-^* characteristic, and the results, in terms of state parameters at the entrance to the barrel ($\bar{x} = 0$) and in the pump tube (reservoir), are given in Table I and Figs. 8 to 11, curves "c"; the characteristic net is shown in Fig. 13. Compared to the isentropic, homogeneous solution (curves "a") the differences are small and amount to less than 10 percent over the range investigated. The mass flow rates, compared in Fig. 14, differ by less than 20 percent.

3.2.2 Real Hydrogen Propellant

The solution for real hydrogen was based on unpublished NBS thermodynamic data, Ref. 5, summarized in Table II. The initial propellant conditions (300°K, 3 atm) were selected to correspond with some of the cycles known to achieve high muzzle velocities (cf., Fig. 18), and an isentropic compression to about 1600°K and 19,000 psia was assumed before start of the projectile motion. For a 0.5-in.-diam, 1-gm projectile, this base pressure results in an acceleration of about 2 million g's.

The basic data required for the characteristic computation are given in Table III, and include functions $\bar{x}_0 = [-\int dp/\rho]/a_0^2$ and

$$\bar{F} = \frac{1}{a_0} \int \frac{dp}{\rho a}. \quad \text{Since for homogeneous, constant acceleration flow}$$

$\bar{\tau}_0 = \sqrt{-2\bar{x}_0}$, this table gives also conditions at the barrel entrance for homogeneous, real hydrogen flow.

The characteristic computation for nonhomogeneous flow was programmed using $\Delta\bar{\tau} = 0.02$ intervals along the C_*^* characteristic and the results, in terms of pressure and temperature at the entrance to the barrel ($\bar{x} = 0$) and in the pump tube, are given in Table IV and Figs. 8 to 11 (curves "d"). The mass flow rates and the characteristic net are shown in Figs. 14 and 15, respectively.

Compared with the ideal ($\gamma = 1.4$) solutions, it is apparent that at large values of $\bar{\tau}_0$, the pressure, temperature, and mass flow ratios are appreciably smaller for real hydrogen. However, in terms of $\bar{\tau}''$ and for $\bar{\tau}'' < 4$, pressures \bar{p}_p differ only slightly between the ideal ($\gamma = 1.4$) and real hydrogen solutions. Also, it is evident from Table III that, in the case of the homogeneous, real hydrogen solution, the Mach number, M , at the barrel entrance differs only very slightly from one, indicating that the homogeneous solution could be closely approximated in a fixed-geometry gun. The reservoir pressure and temperature and the mass flow are in fact practically identical for the homogeneous and non-homogeneous, real hydrogen solutions, Figs. 8 through 11 and 14, curves "d".

SECTION IV GUN PERFORMANCE AND SCALING

In order to examine, in the light of the above results, the limitations of idealized high-speed guns, it is useful to indicate some constraints based on practical design and operational factors and to consider the scaling of launch cycles.

As regards the former, the following can be mentioned:

- (i) Structural properties of the gun define the maximum practical pump tube pressure p_p ; for example, a value of 400 kpsi might be specified.
- (ii) Excessive density and temperature of the propellant would cause unacceptable erosion of the gun components; contamination of propellant with heavy vapors and large heat losses would decrease performance. Maximum acceptable propellant density and temperature cannot be specified, but experience indicates that they are approached in the present high performance guns.

- (iii) The base pressure is limited by the projectile strength.
- (iv) The length/diameter ratio of the barrel is limited in practice to values on the order of 300 because of viscous and frictional losses.
- (v) The minimum projectile volume must be such as to provide adequate sealing of the propellant and stability of motion in the barrel. A length of about one-half caliber appears to be close to the minimum practical value.
- (vi) In general, the severity of the launch cycle used determines the life of gun components, and therefore the maximum performance is related to acceptable operational costs.

Scaling of guns is governed by the similarity parameters for propellant and projectile motion. With perfect gas propellant, and neglecting effects of losses, these are as follows:

$$x/l_0, a_0 t/l_0, p/p_0, \rho/\rho_0, T/T_0, a/a_0, l_0 p_0 / (a_0^2 \rho_p l_p) = \beta p_0 / (a_0^2 \rho_p \epsilon) \quad (30)$$

where a_0, p_0, ρ_0 , etc, are reference parameters of state (e. g., at the projectile base), ρ_p is the projectile density, $l_0 = \beta d$ and $l_p = \epsilon d$ are barrel and projectile lengths, respectively. The factor $\rho_p \epsilon / \beta$ is equal to the projectile mass per unit barrel volume.

For a constant acceleration cycle

$$p_0 = \frac{u^2}{2} \frac{\rho_p \epsilon}{\beta} = \text{projectile kinetic energy per unit barrel volume} \quad (31)$$

4.1 LIMITATIONS OF GUN PERFORMANCE*

In terms of gas-dynamic variables alone, the solution for u, p_p (Fig. 10, real H_2) for a constant acceleration flow indicates that, in a practical case in which the pump tube pressure p_p and the propellant velocity of sound a_0 (i. e., temperature T_0) are restricted to some maximum values, the maximum velocity attainable depends on the minimum acceptable base pressure. However, in view of Eq. (31), the

*In the discussion which follows, vacuum has been assumed in the gun barrel ahead of the projectile, and only the velocity attained during the period of constant acceleration was considered. In practice, a higher velocity would be attained in a longer barrel because of acceleration during the period of base pressure decay.

practical difficulty of decreasing base pressure is immediately apparent. Moreover, the velocity gains which could be realized through decrease of ϵ/β or increase of a_0 and p_p would be reduced by losses which such changes enhance; the possibility of projectile density decrease would depend on matching material strength properties to the base pressure.

In order to gain some insight into the numbers involved in idealized practice (i. e., based on the constant base pressure cycle), muzzle velocity is shown in Fig. 16 in terms of base pressure and projectile specific gravity (Eq. (31)) for a launcher with $\epsilon = 0.5$ and $\beta = 300$. The performance possible with the real hydrogen cycle as given by Fig. 10 with $a_0 = 11,096$ ft/sec ($T_0 = 1600^\circ\text{K}$) and $p_p = 400$ kpsi is indicated by curve "a". As a situation related to practical experience, the point for a Lexan^{®*} projectile (specific gravity 1.2) is marked: it corresponds to a velocity of 38.6 kft/sec and a base pressure of 20 kpsi. The corresponding maximum propellant temperature is 3200°K .

It is interesting to note that this performance comes close to the maximum reported for guns: maximum velocities between 32 and 37 kft/sec have been attained with guns from 0.5 in. to 0.22 in. caliber. The approximate range of projectile weights and velocities currently attainable is shown in Fig. 17, in which data points reported by major laboratories are plotted. Even for weights as small as 0.01 gm, the apparent performance limit does not extend beyond 40 kft/sec. †

Measurements‡ indicate that in the actual high-speed launchings the constancy of the base pressure is only poorly approximated, and maximum base pressures exceeding two or more times the minimum (corresponding to constant acceleration) required have been observed. This is apparent from Figs. 18 and 19, in which typical recorded and calculated, high-speed launch base pressure histories are shown (e. g., for the case of Fig. 18 the maximum base pressure is approximately 3.5 times the constant base pressure value and for Fig. 19 about 7 times). The example discussed above may therefore be regarded as

*Lexan is a polycarbonate resin product of the General Electric Company, Chemical Materials Department, Pittsfield, Mass.

†The boundary corresponding to the 1961 period, as published in Ref. 7, is also shown in Fig. 17. Evidently little progress was made during the last five years.

‡The base pressure is estimated from the x, t measurements of the projectile motion in barrel obtained with the microwave reflectometry, cf., Ref. 6.

the constant base pressure equivalent of the present practice. On the assumption that in the future constant acceleration cycles could be more closely approximated, some possibilities of attainment of higher speeds are discussed next in quantitative terms. The specific solution obtained for real hydrogen (Fig. 10) was assumed to apply (in dimensionless form) in all cases considered.

A launch cycle limited to certain maximum values of p_p and a_0 offers no possibility of increased velocity, unless projectiles of smaller density can be used and/or the parameter ϵ/β decreased, but does allow lower velocities with denser and longer projectiles. In the particular case of the launch cycle represented by curve "a", Fig. 16, a 50-kft/sec velocity could be reached with a 9.3-kpsi base pressure with the following projectile-gun combinations:

Specific Gravity	ϵ	β	Relative Launch Duration*
1.2	1/3	728	1.85
0.6	1/3	364	0.93
1/3	1/2	300	0.76

*Normalized by the launch duration for Lexan at 38.6 kft/sec, curve "a", Fig. 16.

It is seen that, for the density of Lexan (1.2), in spite of a shorter projectile ($d/3$), a very long barrel (728 d) would be required; moreover, the duration of launch as compared with the 38.6-kft/sec case, would increase (as would, e. g., heat losses) by 85 percent. More practical projectile/gun configurations correspond to a lower density range in which, as will be discussed later, sufficiently strong materials are not available.

Higher performance launch cycles are indicated in Fig. 16 by curves "b" and "c"; curve "b" corresponds to a maximum pump tube pressure of 800 kpsi (rather than 400 kpsi for curve "a"), whereas curve "c" is drawn for double the propellant temperature (or $a_0 = 15.7$ kft/sec). Either of these changes results in attainment of higher velocity at a given projectile density and gun/projectile configuration. For example, a velocity 47.2 kft/sec is obtained with Lexan by doubling the initial propellant temperature. The maximum propellant temperature is increased by 85 percent, to 5920°K, and the base pressure by 50 percent, to 30 kpsi.

Current experience indicates that, provided the constant base pressure cycle is more closely approached, gains in velocity may be possible through such higher performance cycles. It is apparent that in the launches which are close in performance to the 38.6-kft/sec Lexan shot (Fig. 16, curve "a"), base pressures and maximum propellant pressures and temperatures are considerably exceeded over the idealized, constant pressure values, while satisfactory projectile integrity and acceptable rate of deterioration of gun components are maintained. It should therefore be possible to apply such extreme conditions also to the constant pressure cycles, and thus increase muzzle velocity.

As regards projectile materials, the advantage offered by Lexan (or other strong plastics in the specific gravity range of one) is indicated by Fig. 16. On the assumption that the maximum base pressure to which any material can be subjected is related to its strength properties (ultimate tensile and yield stress), the areas occupied by various materials are shown, covering the range from plastics to high strength steels.

No materials of low density, with which high speeds could be attained at low base pressures, appear available. From experimental measurements* it is known that Lexan is capable of withstanding base pressures as high as 125 kpsi, and therefore, provided launch cycles utilizing higher pressures and temperatures are perfected, this material offers the possibility of attaining higher maximum speeds than are now available, or launching heavier projectiles at lower speeds. In view of the indicated "dynamic strength" of Lexan, the application of light metals (e. g., Mg, Li, Be, Al, and their alloys) offers no advantage in terms of velocity; other high strength materials (Ti, steels) fall outside of the useful density range.

4.2 LINEAR SCALING OF GUNS

The application of a given launch cycle, capable of a specific velocity at a certain base pressure, to guns of different calibers is of practical interest. Equation (31) indicates that the gun performance will remain unchanged provided the quantity $\epsilon \rho_t / \beta$ remains constant, and assuming a scaling of the effects of losses. Thus, for a given projectile density or material (which would be expected to remain unchanged,

*The base pressure is estimated from the x, t measurements of the projectile motion in barrel obtained with the microwave reflectometry, cf., Ref. 6.

having to sustain the same base pressure or stress), the projectile length and its weight per unit bore area ($\epsilon d \rho_p$) scale linearly with caliber*, as does the barrel length (βd).

In practical applications to high-speed guns, the first stage is similarly scaled by keeping the ratio

$$l_p \rho_p / l_{pt} = \text{piston mass/pump tube volume}$$

constant, as well as the piston velocity, the gas-dynamic parameters (i. e., the initial propellant charge pressure and temperature), and the projectile release pressure. Since large piston lengths are involved, it is often preferable to increase average piston density as the caliber increases, rather than increase the piston length.

The interest in the scaling of guns stems from the possibility of developing high performance launchers on small scale and applying the results to larger calibers, thus avoiding costly and time consuming, large-scale experimental programs. The validity of linear scaling was recently examined in the VKF, and the results are shown in Figs. 18 and 19.

In Fig. 18 the measurements[†] of base pressure made on two shots are compared with the values calculated by the VKF digital program. The data were obtained with a 0.5-in. -caliber gun; the other parameters are indicated in Fig. 18. Except for the peak base pressure, the agreement between observation and calculation is good, both with respect to the history of the base pressure and the muzzle velocity.

Equally satisfactory comparisons were obtained for a wide variety of launch velocities and gun calibers (0.375 to 2.5 in.), and on this basis the VKF computational method is considered adequate for use in examination of linear scaling of guns.[‡] The results of scaling of a 0.375-in. -caliber gun cycle to 0.5 and 2.5-in. caliber sizes are shown in Fig. 20. The departures from the exact linear scaling in the

*If the restriction on density or ϵ or both were lifted, the caliber alone could be varied, $d \propto 1/(\epsilon \rho_p)$, irrespective of the barrel length.

[†]The base pressure is estimated from the x, t measurements of the projectile motion in barrel obtained with the microwave reflectometry, cf., Ref. 6.

[‡]The VKF computational method allows for real-gas thermodynamics, gas and piston friction, and plastic deformation of piston in the pump tube-barrel transition section.

parameters as used are noted in Table V. The 2.5-in. -caliber gun was scaled exactly from the 0.375-in. -caliber gun. The 0.5-in. -caliber gun, an existing one, closely approximated linear scaling of the 0.375-in. -caliber gun, but had a different shape of the pump tube-launch tube transition; also, a slightly lower release pressure was assumed and estimated. The main difference was in the higher piston velocities in the case of the 0.5-in. -caliber gun, which resulted in higher peak base pressure and higher launch velocity. However, excellent agreement was obtained for the 0.375-in. - and 2.5-in. -caliber guns, i. e., over a linear scale range of 6.67, for which the same piston velocity was used. The linear scaling principle was also confirmed, in terms of muzzle velocity, by performance measured with 0.375-in. - and 0.5-in. -caliber launchers at the 30-kft/sec level, using the cycle of Figs. 18 and 19.

In Table V the maximum computed pump tube pressure is also given. The value of this pressure is critically dependent on the shape of transition between the pump tube and barrel. Although good agreement is indicated for the 0.375-in. - and 2.5-in. -caliber launchers (geometrically identical guns), a much higher pressure is indicated for the 0.5-in. -caliber gun, presumably because of a more abrupt transition in this launcher.

It is of interest to examine the present state of the art in terms of linear scaling. Figure 17 clearly indicates that in general practice the linear scaling of guns has not been realized, the maximum velocity boundary showing a decrease with increasing projectile weight or caliber. For example, the application of linear scaling to a 1-gm, 32-kft/sec launch with a 0.5-in. -caliber gun indicates the possibility of a 1-kg launch at the same speed from a 5-in. -caliber gun, whereas the actual record for this weight is below 20 kft/sec. This situation reflects practical difficulties in scaling up hardware subjected to extreme pressures, mounting costs, and a technological lag between availability of experimental, small-scale equipment and large-scale facilities. It is clear that optimization of launch cycles toward the constant pressure ideal, and corresponding reduction of extreme cycle pressures, would facilitate development of large, high-speed guns.

SECTION V CONCLUSIONS

Solutions for isothermal, isentropic, and constant Mach number (at a specified location) flows with constant acceleration are obtained.

It is shown that in application to high-speed guns, these solutions necessitate variable gun geometry or heating of the propellant; both requirements are considered at present impractical. Numerical solutions which give constant projectile acceleration in a fixed-geometry gun are computed for ideal and real hydrogen propellant. Using the latter, and the appropriate similarity parameters, as well as practical constraints related to gun and projectile geometry and strength, it is shown that a substantial increase in muzzle velocity could be obtained if the constant base pressure cycle were more closely approximated in actual launchings.

At present the velocity attained with large caliber guns is much smaller than with the small ones. In this connection, the validity of linear scaling of guns and the resulting possibility of application of small-scale developments to large caliber guns are indicated.

REFERENCES

1. Prandtl, L. Essentials of Fluid Dynamics. Blackie & Son Ltd., London, 1952, p. 14 et seq.
2. Stanyukovitch, K. P. Unsteady Motion of Continuous Media. Pergamon Press, 1960, pp. 605-607.
3. Smith, F. "Theory of a Two Stage Hypervelocity Launcher to Give Constant Driving Pressure at the Model." Journal of Fluid Mechanics, V. 17, Pt. 1, 1963, pp. 113-125.
4. Oswatitsch, K. Gas Dynamics. Chapter 3, Academic Press, Inc., New York, 1956.
5. Wooley, H. Private Communication, National Bureau of Standards, Washington, D. C., 1965.
6. Clemens, P. L. and Hendrix, R. E. "Development of Instrumentation for the VKF 1000-ft Hypervelocity Range." Advances in Hypervelocity Techniques, Proceeding of the Second Symposium on Hypervelocity Techniques, Plenum Press, New York, 1962, p. 245.
7. Nelson, W. C. (Editor). The High Temperature Aspects of Hypersonic Flow. Pergamon Press, Round Table Discussion, Fig. 5, p. 760 (contribution by J. Lukasiewicz), 1963.

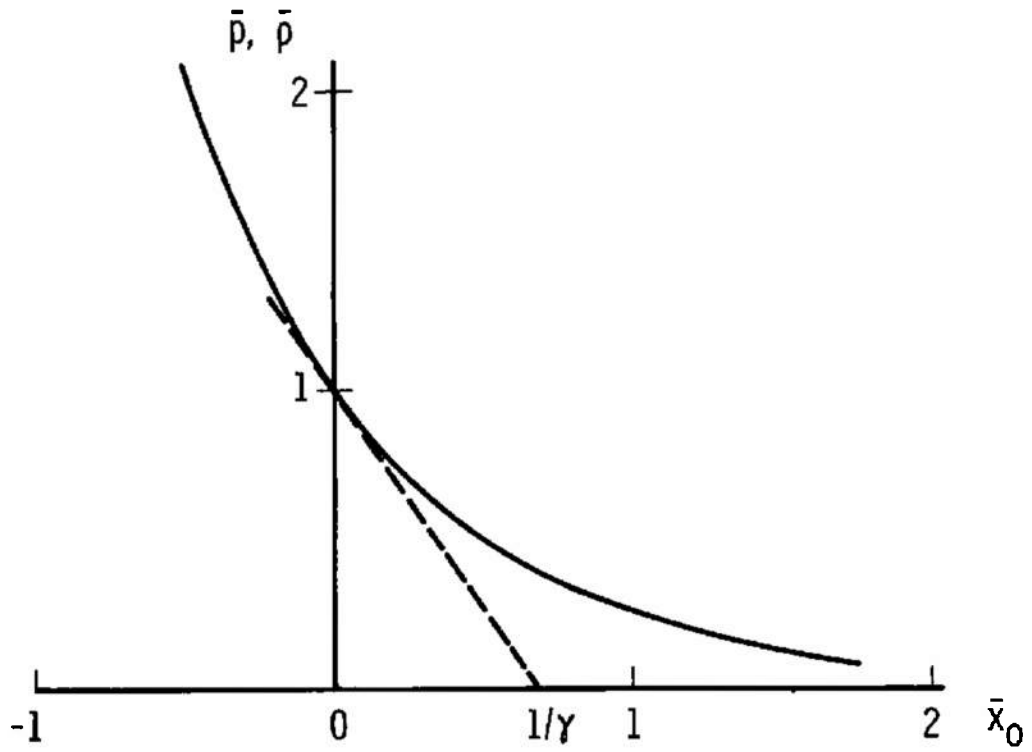


Fig. 1 Pressure and Density Distribution in Isothermal Flow
(Isothermal Atmosphere, $\gamma = 1.4$)

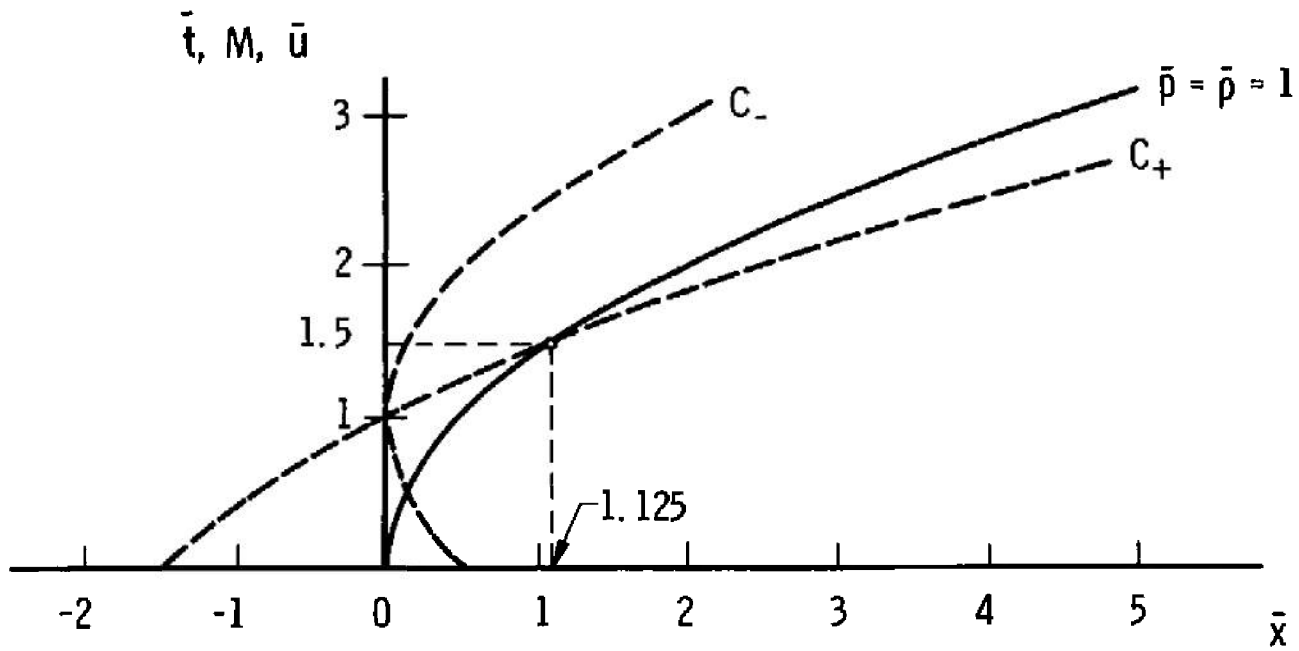


Fig. 2 Isothermal Flow

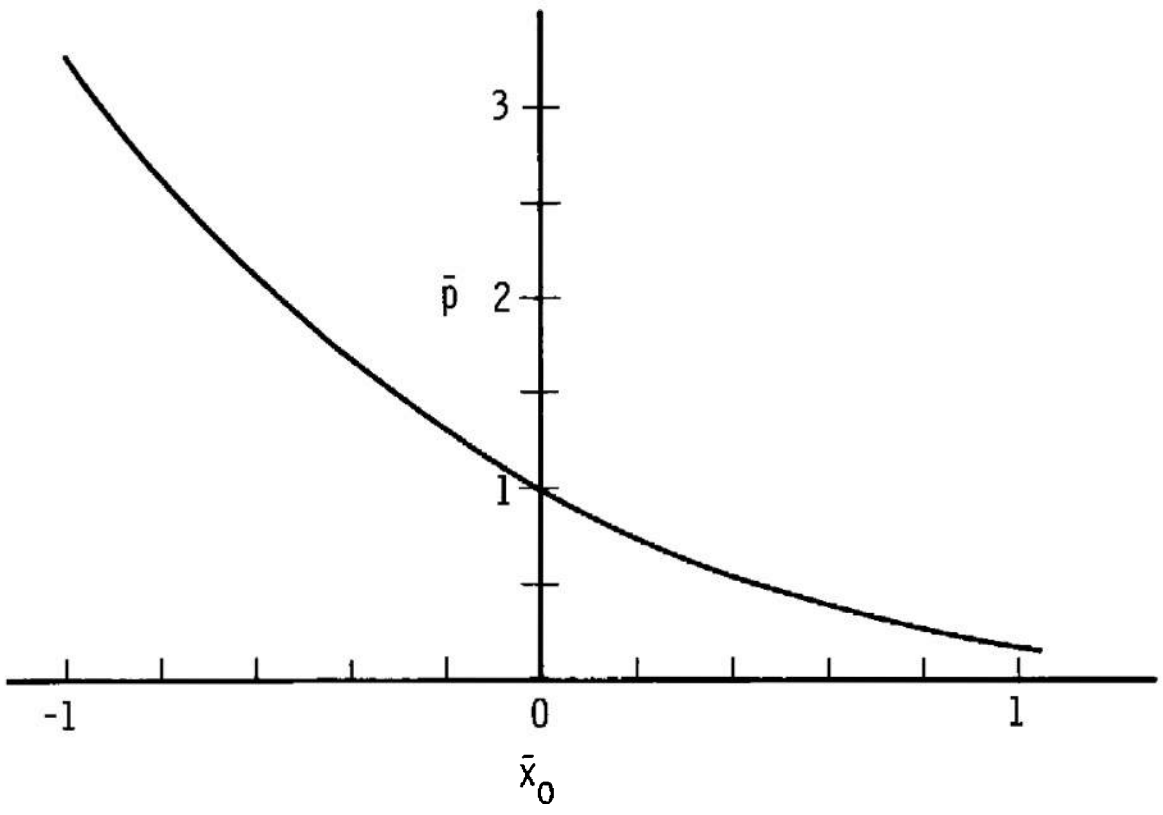
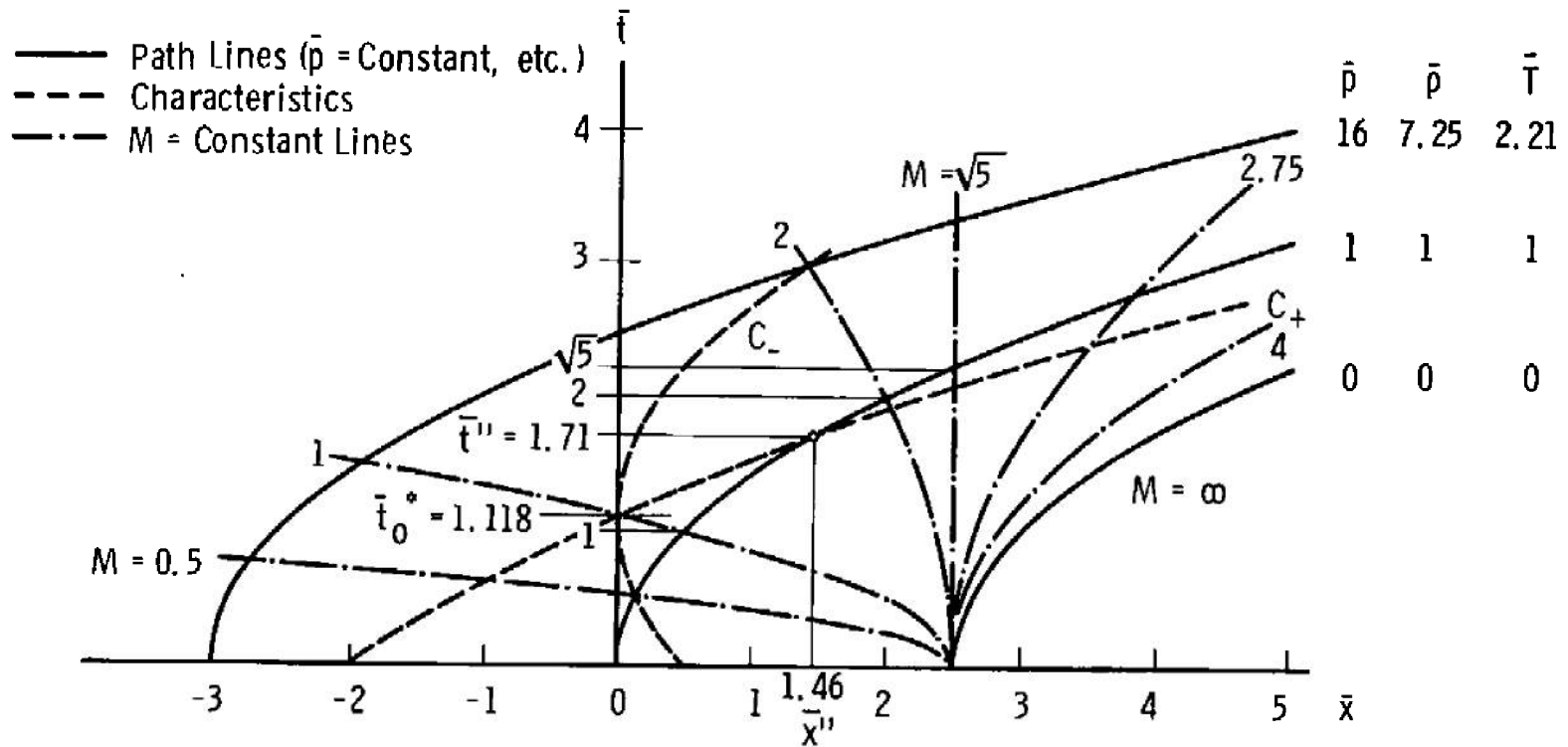


Fig. 3 Pressure Distribution in Isentropic Flow ($\gamma = 1.4$)

Fig. 4 Isentropic Flow ($\gamma = 1.4$)

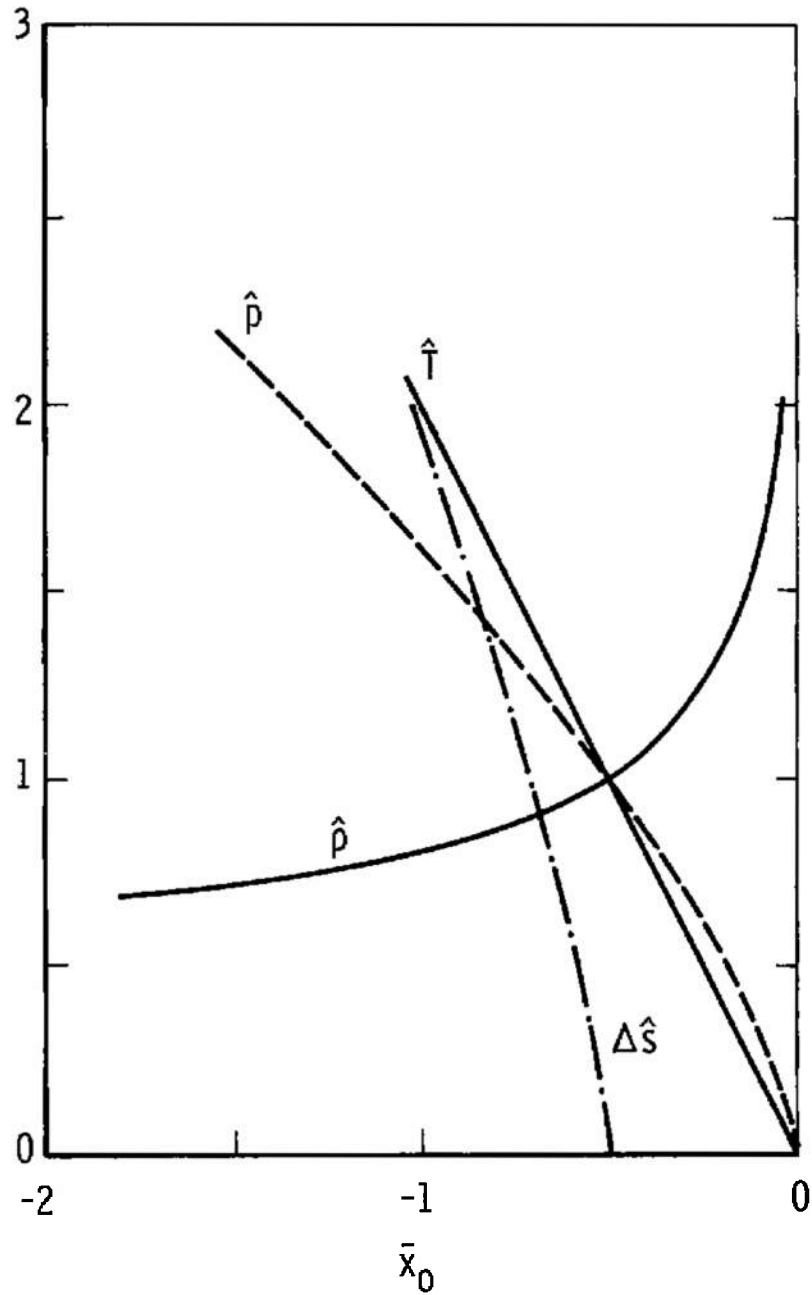


Fig. 5 Distribution of Parameters of State for Flow with $M_0 = 1$ ($\gamma = 1.4$)

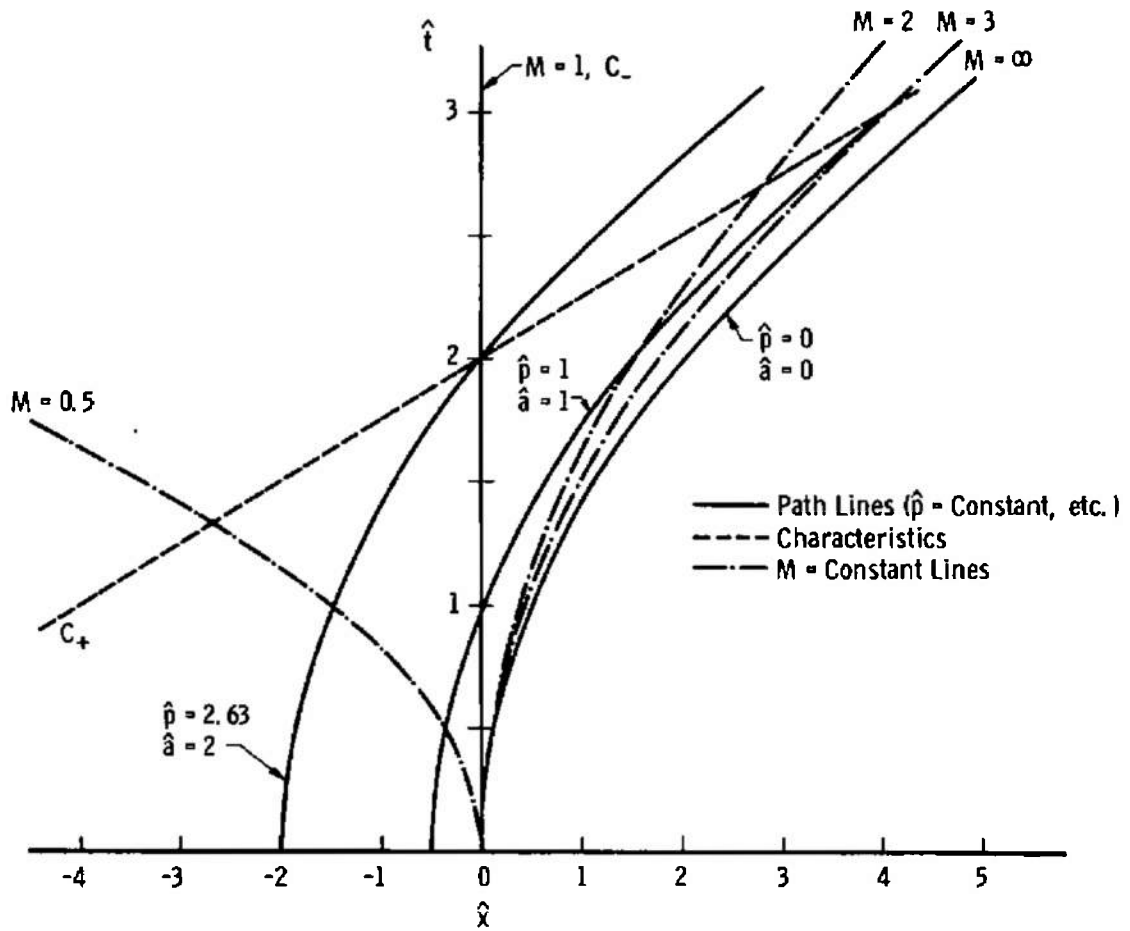


Fig. 6 Flow with $M_0 = 1$ ($\gamma = 1.4$)

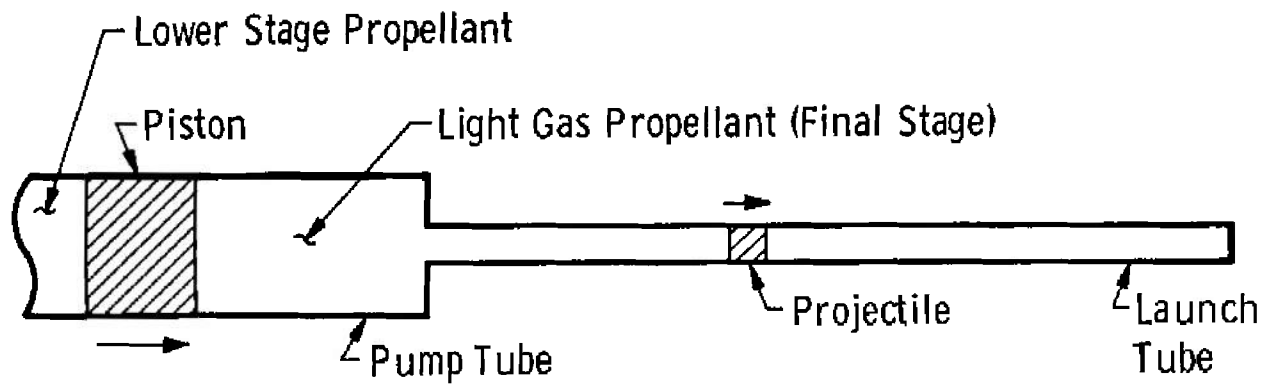


Fig. 7 Typical Gun Configuration (Final Stage of a Light-Gas Gun)

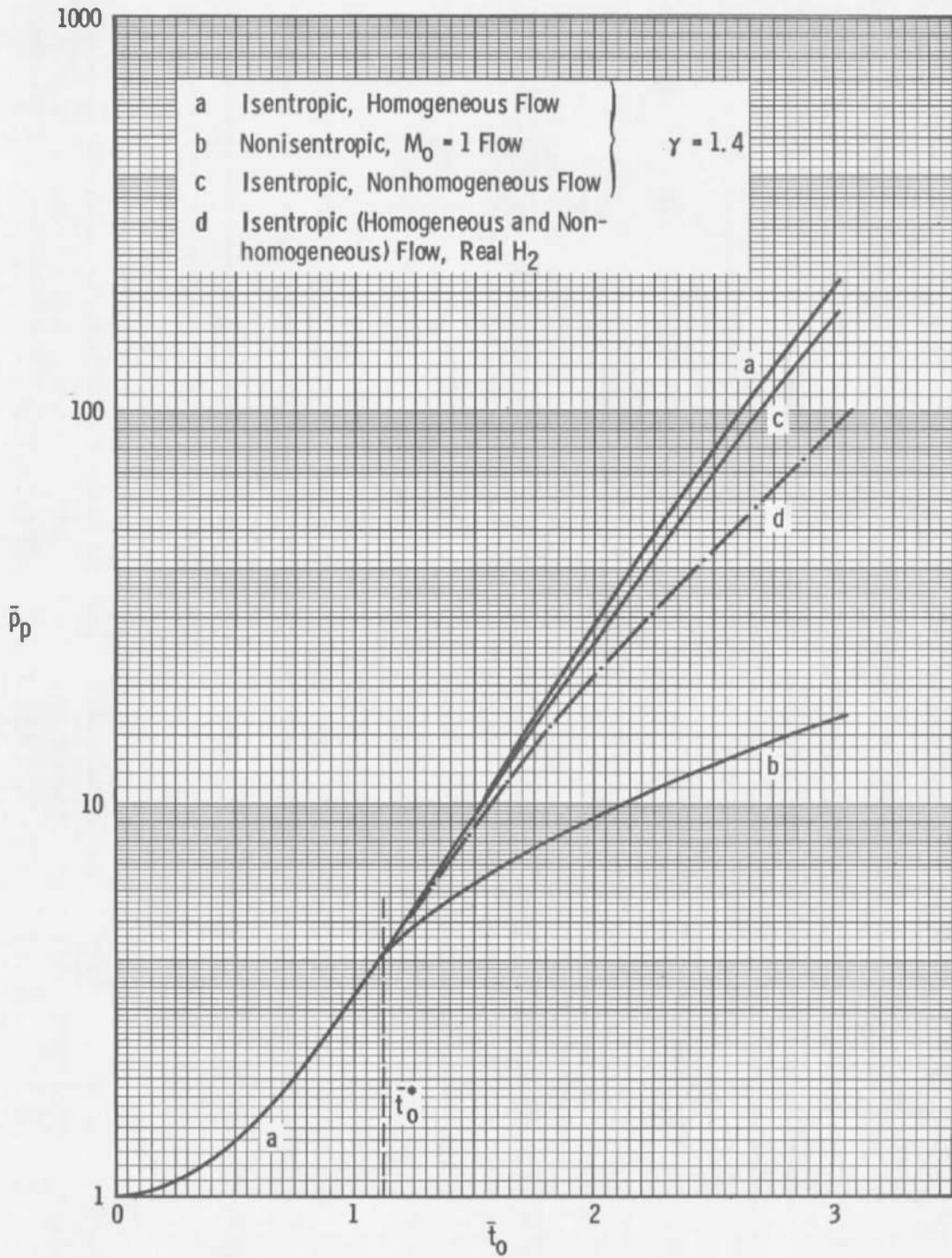


Fig. 8 Variation of Pump Tube Pressure with Time

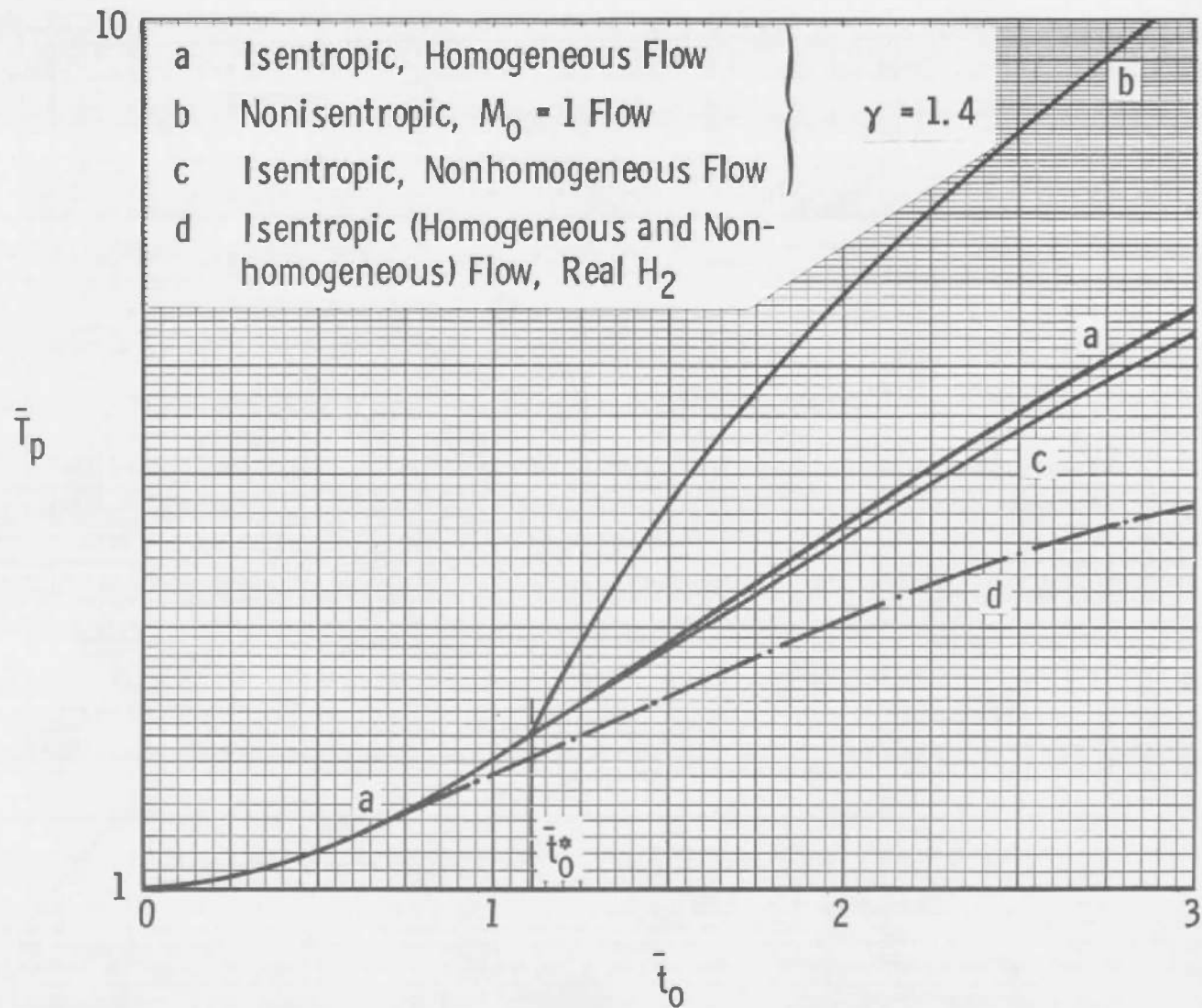


Fig. 9 Variation of Pump Tube Temperature with Time

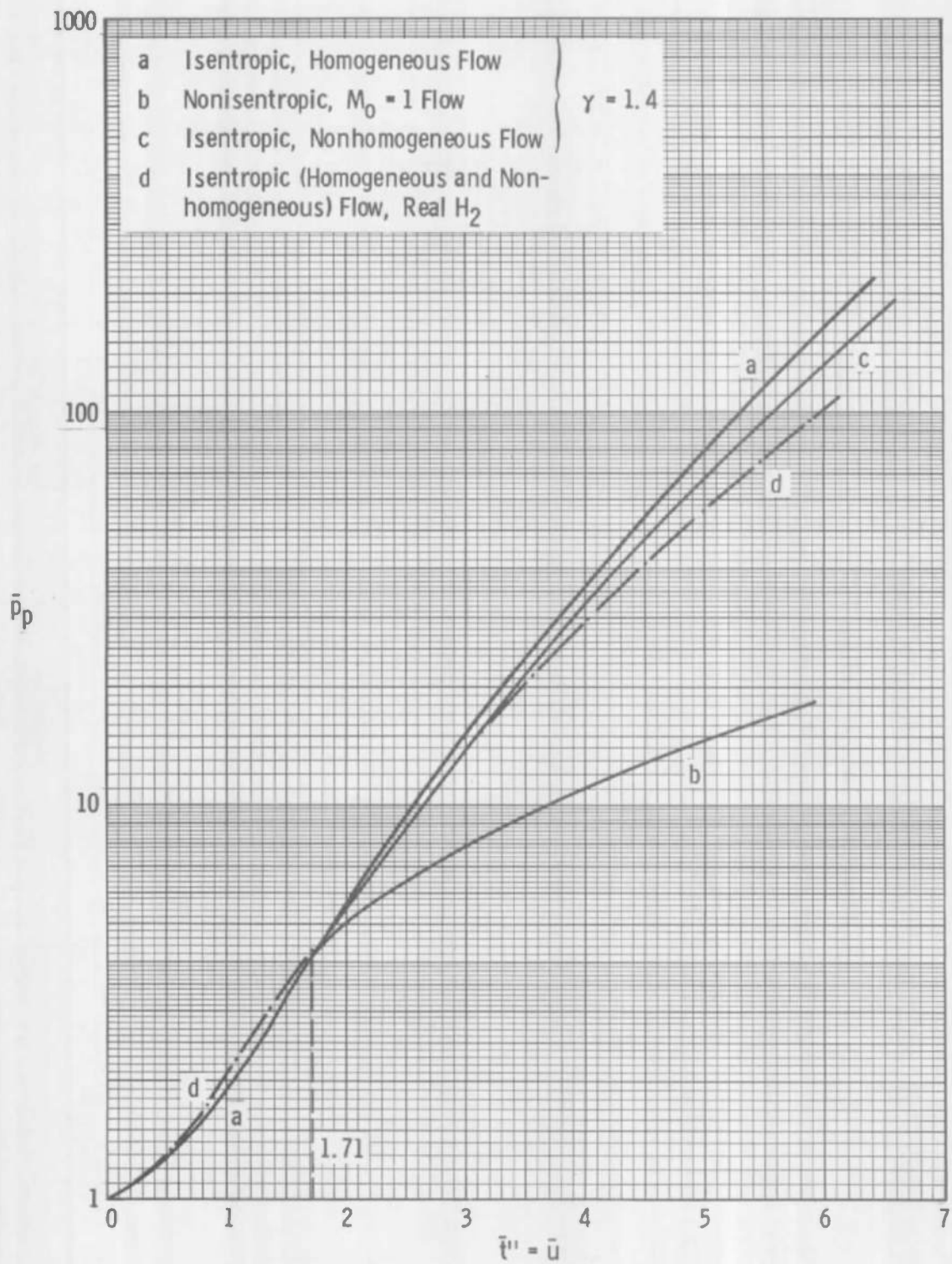


Fig. 10 Variation of Pump Tube Pressure with Characteristic Time $\bar{\tau}''$

- a Isentropic, Homogeneous Flow
 - b Nonisentropic, $M_0 = 1$ Flow
 - c Isentropic, Nonhomogeneous Flow
 - d Isentropic (Homogeneous and Non-homogeneous) Flow, Real H_2
- } $\gamma = 1.4$

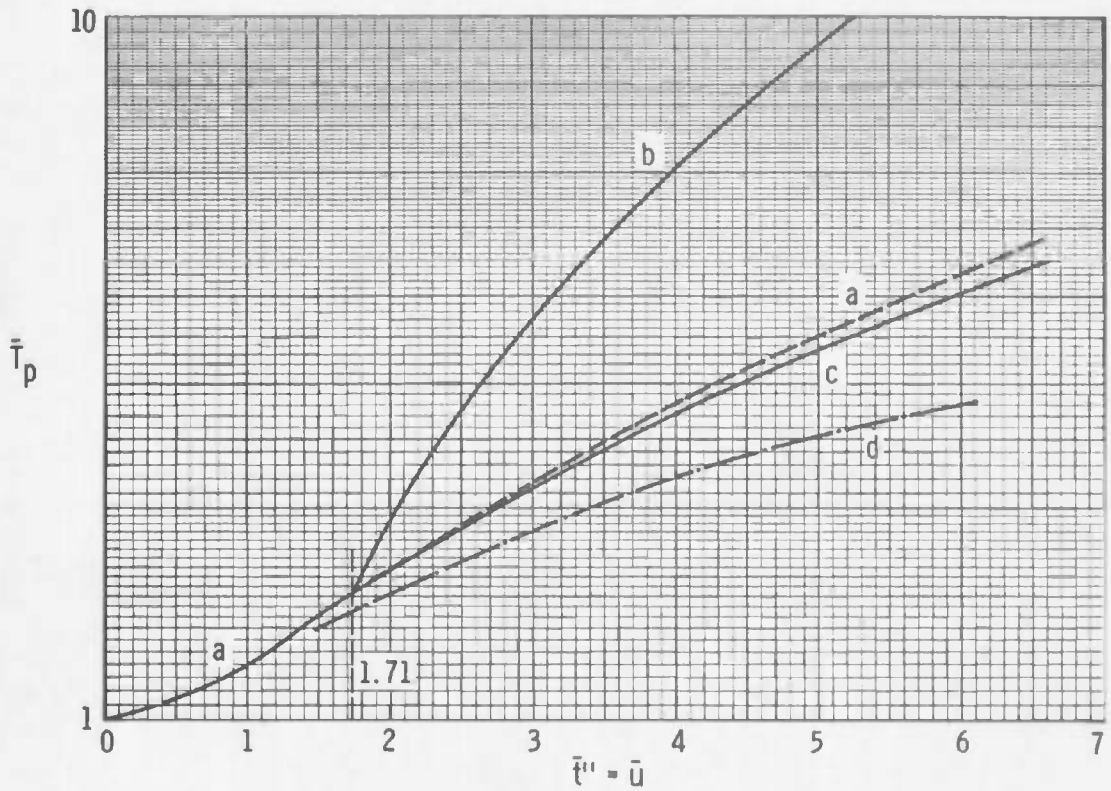


Fig. 11 Variation of Pump Tube Temperature with Characteristic Time t''

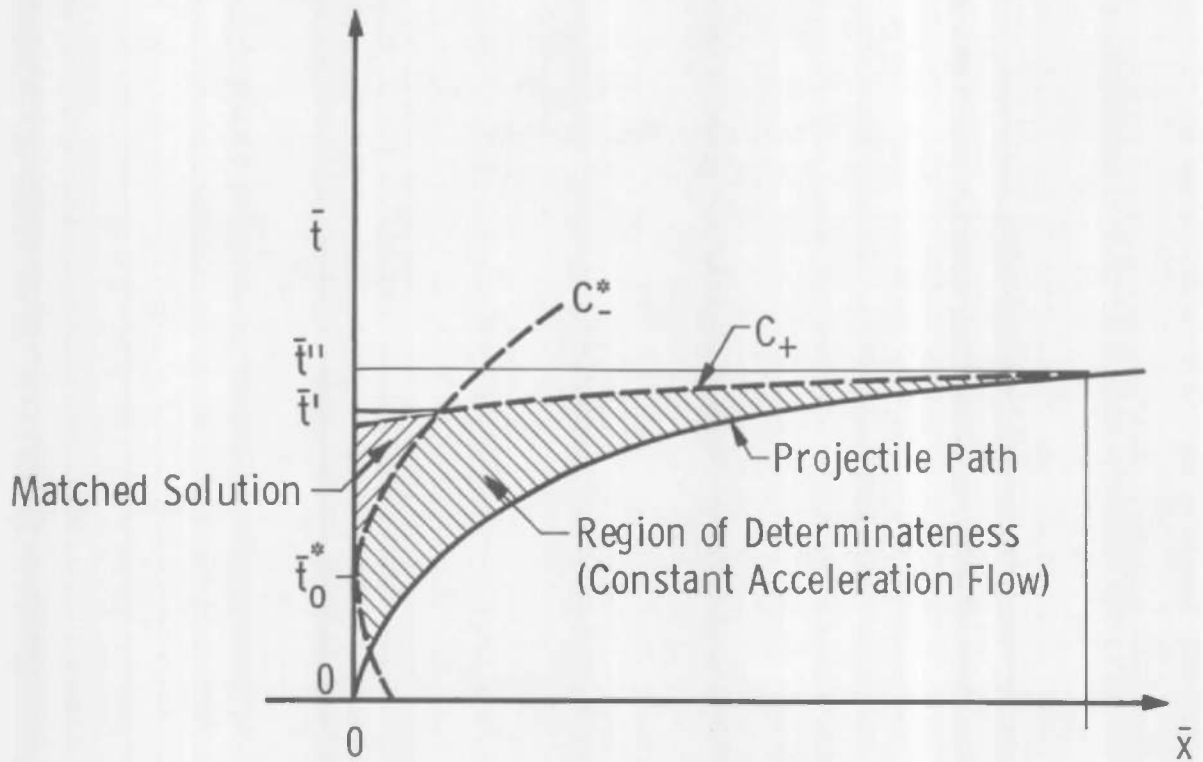


Fig. 12 Nonhomogeneous Solution for Constant Geometry and Acceleration, Isentropic Launch Cycle

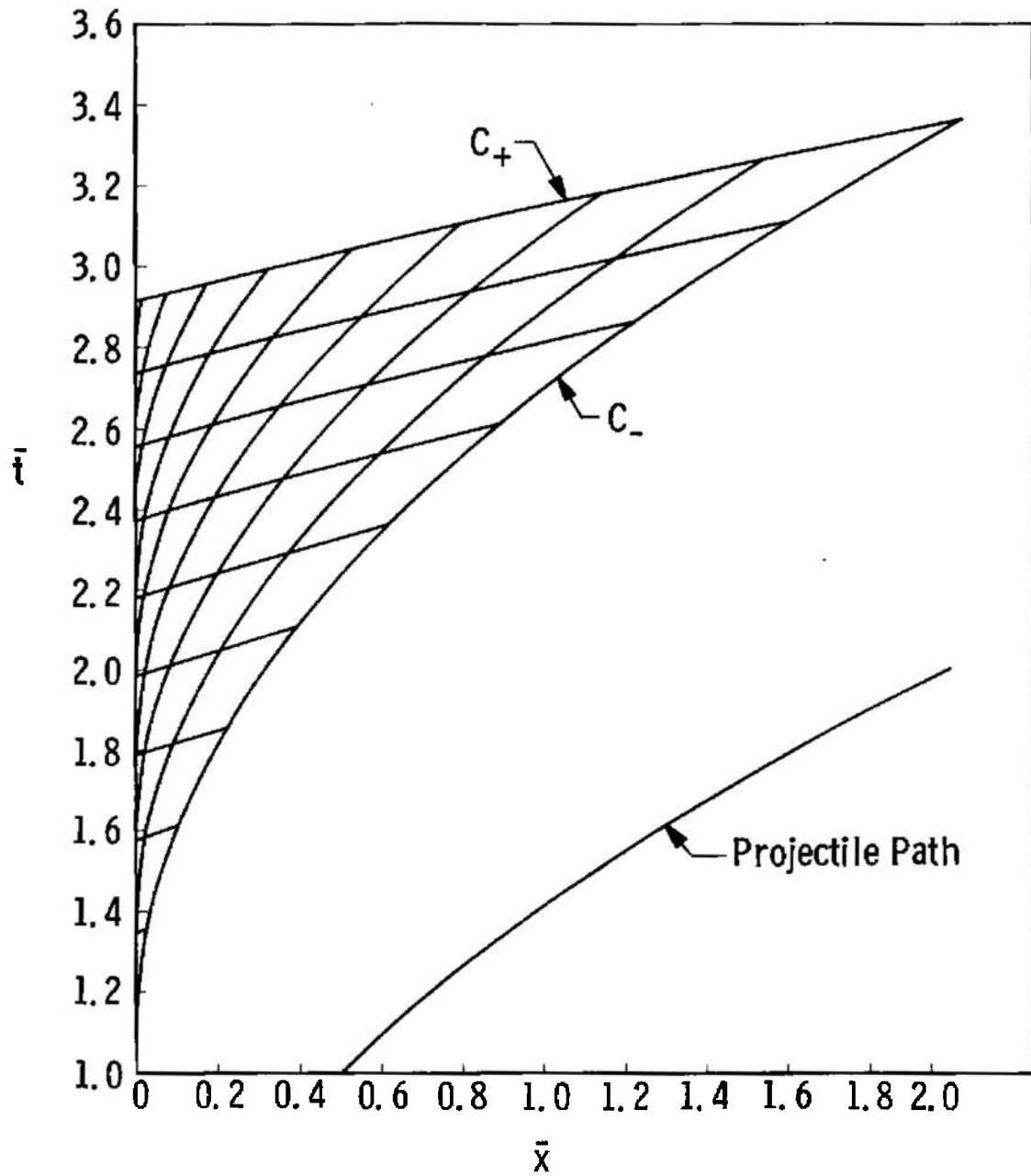


Fig. 13 Characteristic Solution of Nonhomogeneous, Isentropic Flow ($\gamma = 1.4$)

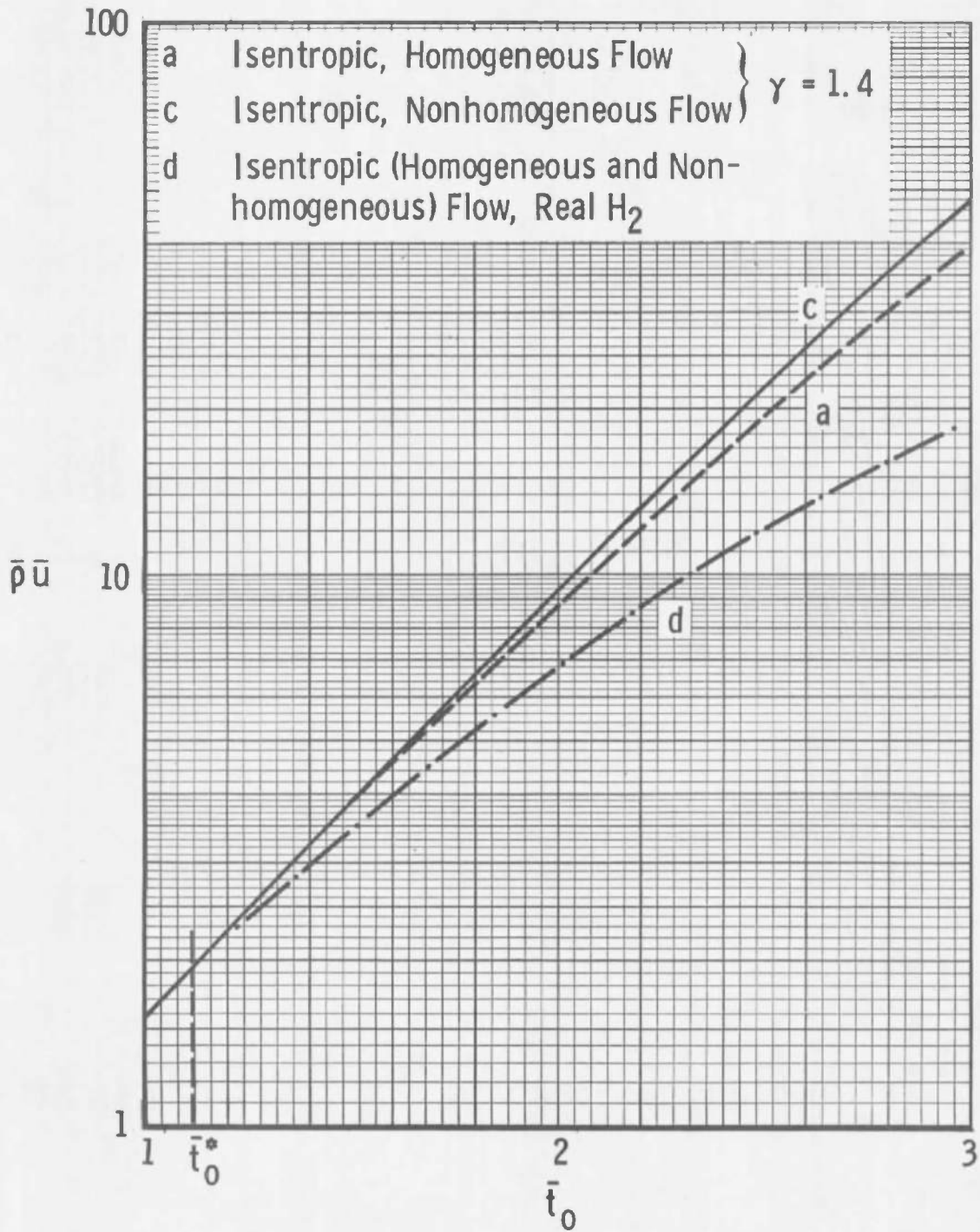


Fig. 14 Rates of Mass Flow for Homogeneous and Nonhomogeneous, Isentropic Solutions

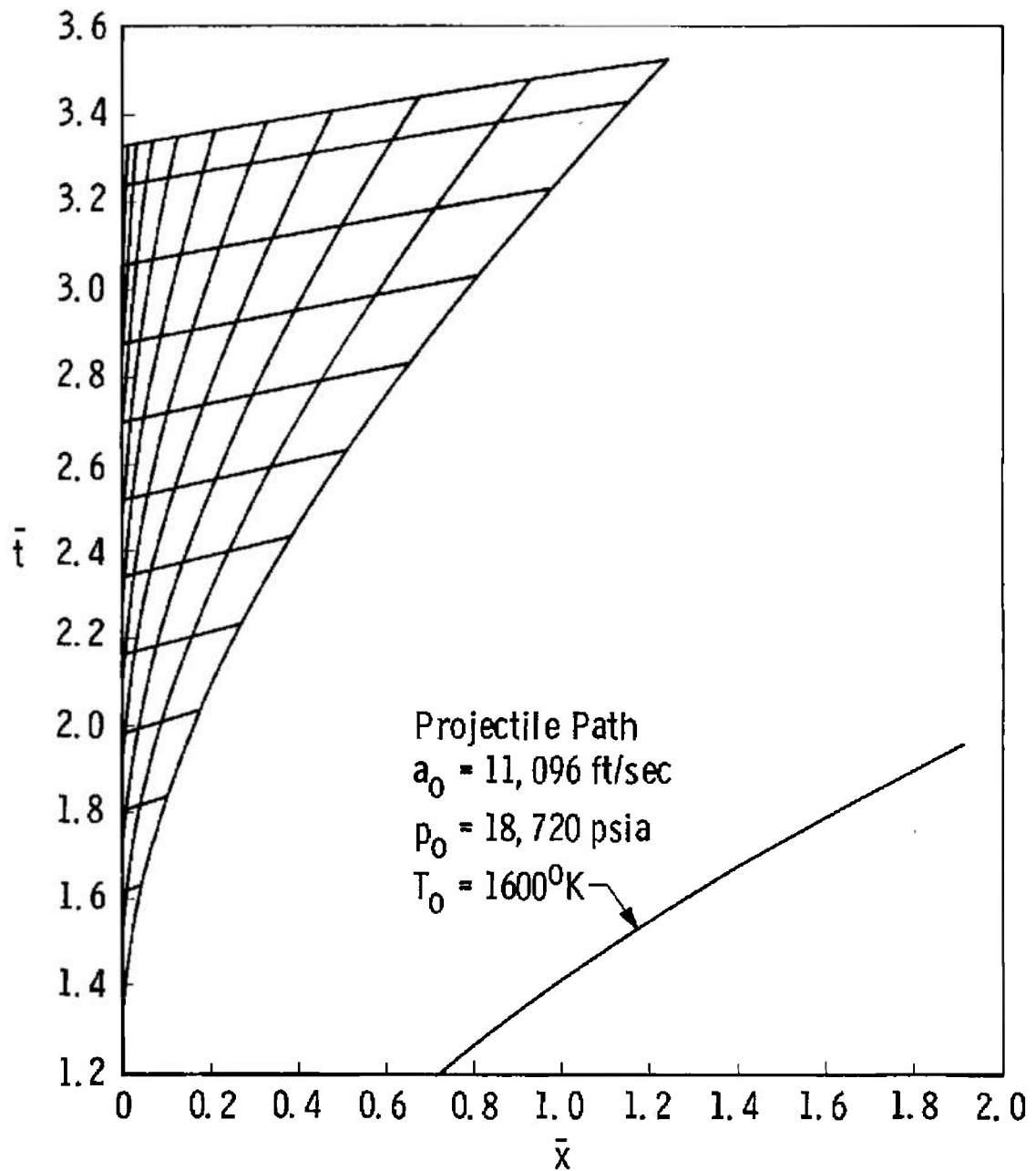


Fig. 15 Characteristic Solution of Nonhomogeneous Flow of Real Hydrogen

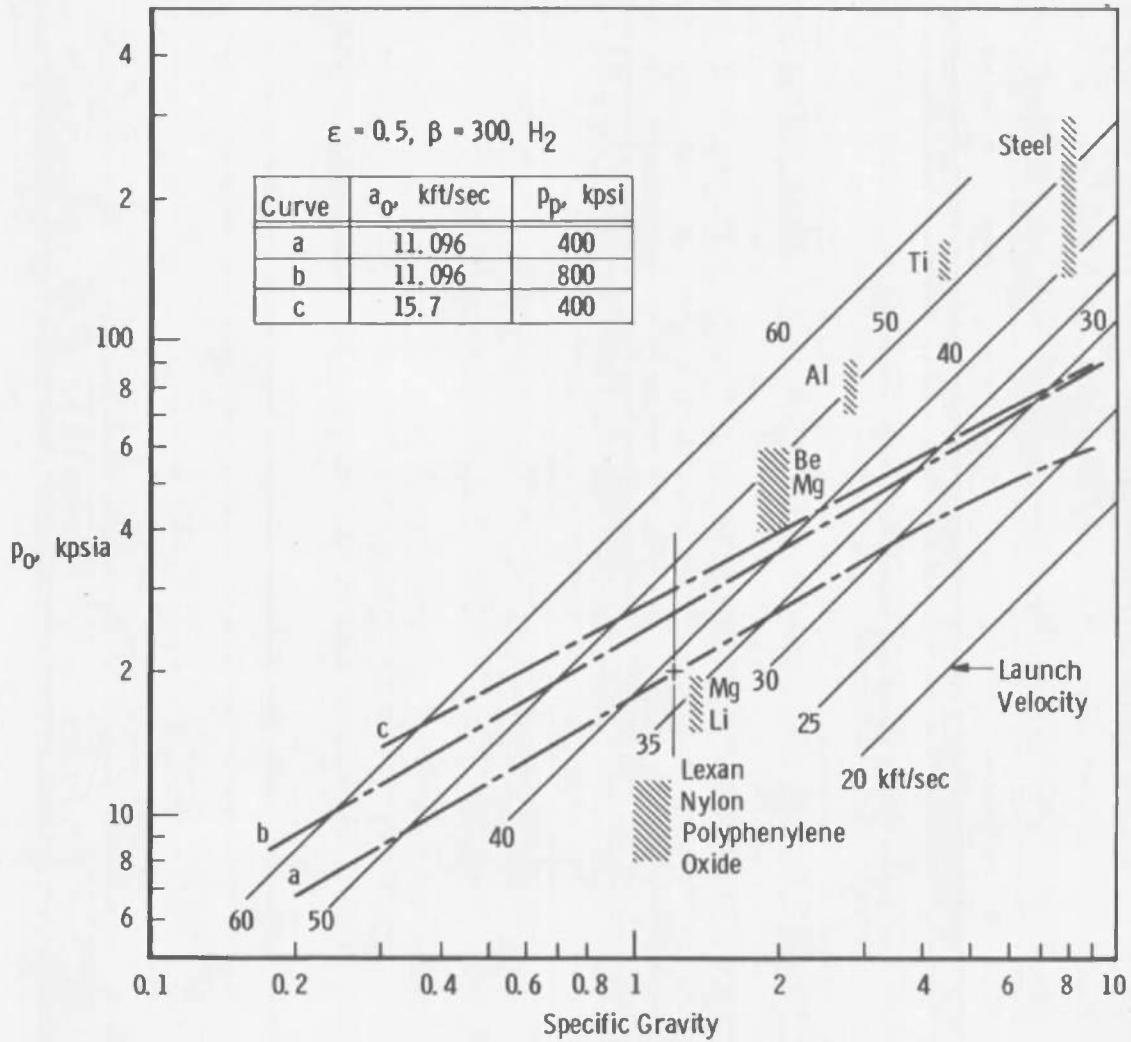


Fig. 16 Performance of Guns and Materials

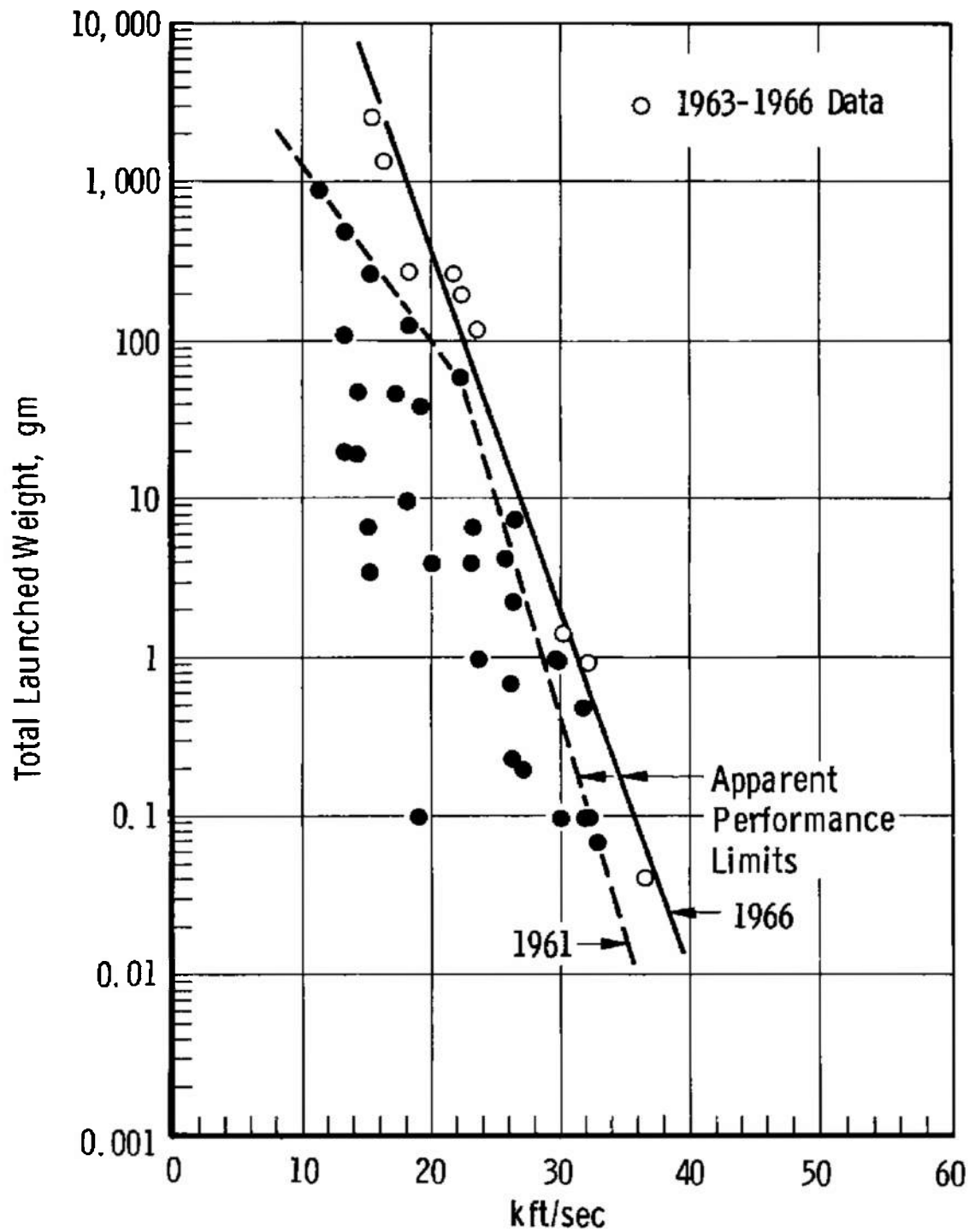


Fig. 17 Maximum Launch Velocities and Weights

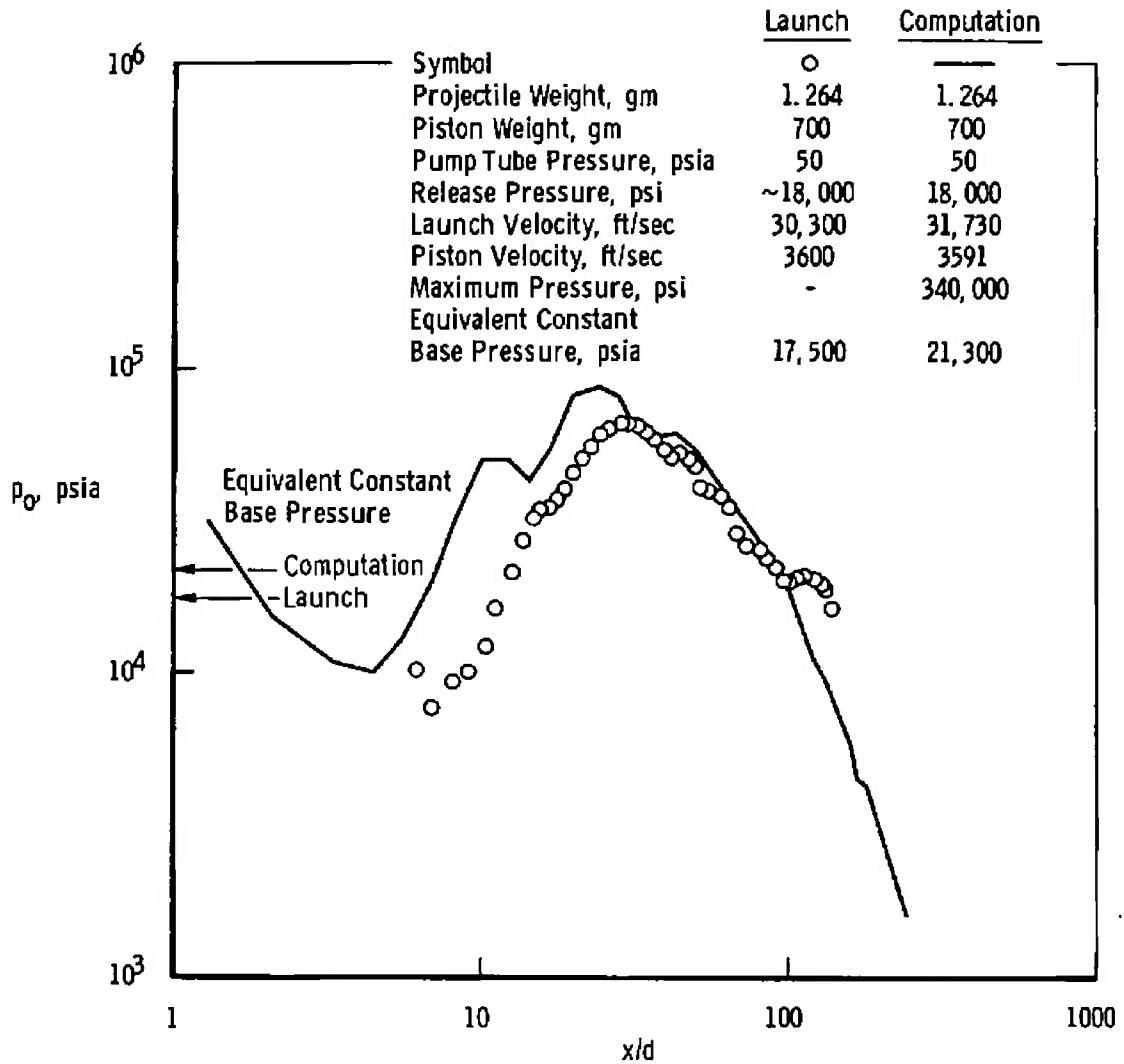


Fig. 18 Measured and Computed Base Pressure in a 0.5-in.-caliber Gun (Low Base Pressure Peak)

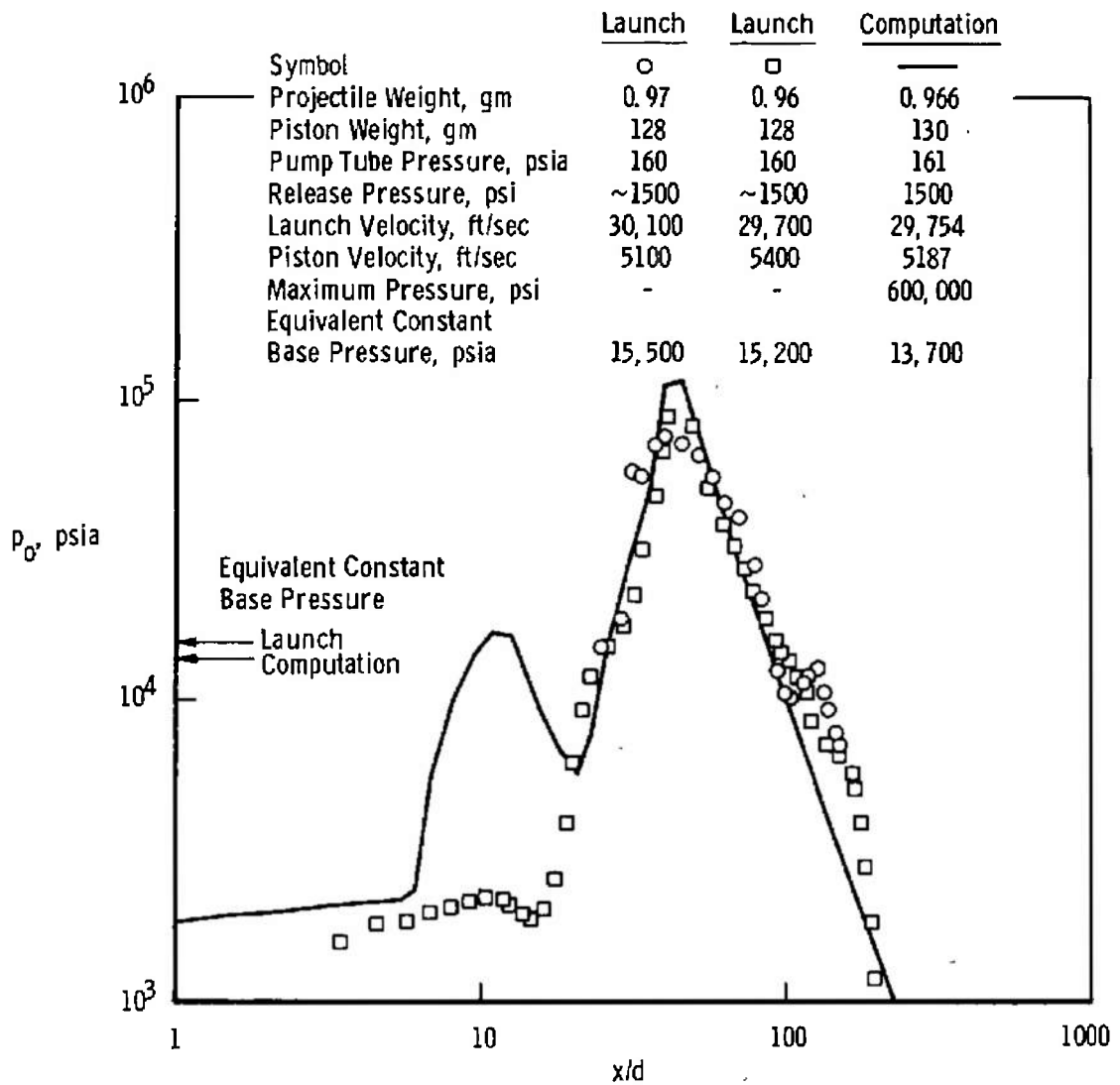


Fig. 19 Measured and Computed Base Pressure in a 0.5-in.-caliber Gun (High Base Pressure Peak)

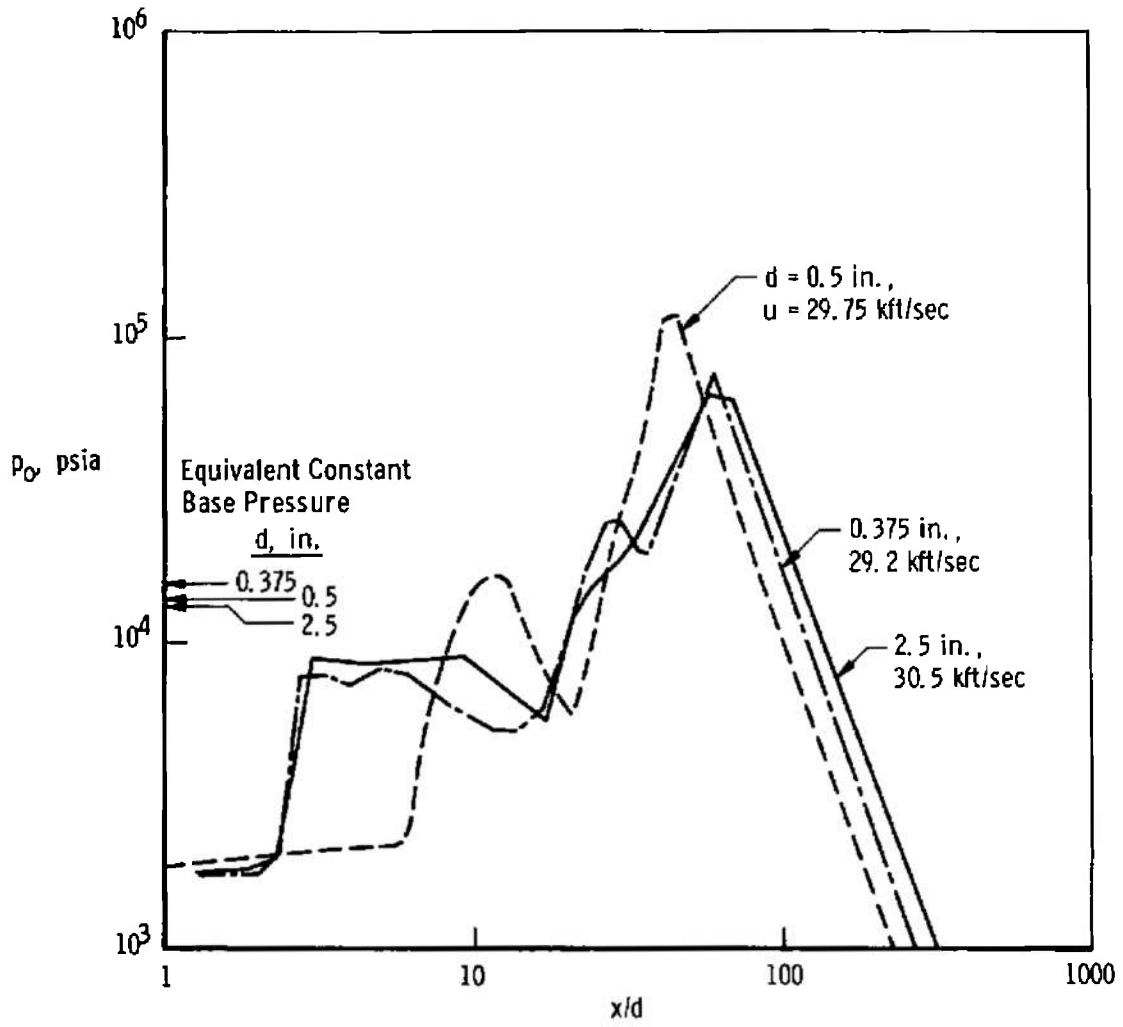


Fig. 20 Computed Base Pressures for Linearly Scaled Guns

TABLE I
ISENTROPIC FLOW, $\gamma = 1.4$

\bar{t}_0	\bar{t}''	At $\bar{x} = 0$					\bar{T}_p	\bar{p}_p
		\bar{a}	\bar{T}	\bar{p}	$\bar{\rho}$	$\bar{\rho}u$		
Isentropic, homogeneous flow								
0	0	1.000	1.000	1.000	1.00	0	1.000	1.000
0.2	0.22	1.004	1.008	1.029	1.021	0.204	1.016	1.057
0.4	0.48	1.016	1.032	1.116	1.081	0.433	1.064	1.242
0.5	0.63	1.026	1.050	1.186	1.129	0.565	1.100	1.396
0.6	0.775	1.035	1.072	1.275	1.189	0.714	1.144	1.602
0.8	1.110	1.062	1.129	1.524	1.351	1.081	1.256	2.220
1.0	1.475	1.095	1.200	1.893	1.577	1.577	1.400	3.247
1.118	1.708	1.118	1.25	2.184	1.747	1.953	1.500	4.134
1.5	2.525	1.205	1.45	3.676	2.53	3.8	1.9	9.45
2	3.710	1.34	1.8	7.812	4.34	8.68	2.6	28.25
2.5	5	1.5	2.25	17.09	7.58	18.95	3.5	80
3	6.36	1.67	2.8	36.76	13.1	39.3	4.6	208
Isentropic, nonhomogeneous flow ($M_{\bar{x}=0} = 1$)								
1.358	2.208	1.201	1.44	3.612	2.502	3.004	1.73	6.837
1.582	2.708	1.285	1.65	5.775	3.497	4.494	1.98	10.93
1.793	3.208	1.368	1.87	8.967	4.788	6.550	2.24	16.97
1.995	3.708	1.451	2.10	13.56	6.433	9.335	2.52	25.68
2.190	4.208	1.535	2.35	20.05	8.51	13.06	2.83	37.95
2.380	4.708	1.618	2.62	29.03	11.08	17.92	3.14	54.95
2.564	5.208	1.701	2.89	41.26	14.24	24.22	3.47	78.10
2.745	5.708	1.785	3.18	57.66	18.08	32.28	3.82	109.15
2.923	6.208	1.868	3.48	79.36	22.71	42.43	4.18	150.24
3.000	6.428	1.905	3.62	90.93	25.03	47.69	4.35	172.13

TABLE II
HYDROGEN THERMODYNAMIC DATA FOR $s/R = 16$, $T = 100$ (100) 3900°K (Ref. 5)

T, °K	$\log_{10} \rho$ (amagat)	$\log_{10} p$ (atm)	$\log_{10} H/R$ (°K)	γ	$a/4120.8$	Z	H/RT	Z*
100.	-5.8046-01	-1.0171 00	2.5820 00	1.5008 00	6.2647-01	9.9997-01	3.8192 00	10.0000-01
200.	2.1042-02	-1.1438-01	2.8358 00	1.4678 00	8.7639-01	1.0005 00	3.4261 00	10.0000-01
300.	4.4115-01	4.8238-01	3.0108 00	1.4140 00	1.0542 00	1.0018 00	3.4171 00	10.0000-01
400.	7.5178-01	9.1890-01	3.1385 00	1.4055 00	1.2149 00	1.0040 00	3.4389 00	10.0000-01
500.	9.9410-01	1.2595 00	3.2378 00	1.4076 00	1.3615 00	1.0073 00	3.4581 00	10.0000-01
600.	1.1921 00	1.5386 00	3.3191 00	1.4118 00	1.4970 00	1.0117 00	3.4746 00	10.0000-01
700.	1.3594 00	1.7753 00	3.3880 00	1.4169 00	1.6243 00	1.0173 00	3.4907 00	10.0000-01
800.	1.5046 00	1.9815 00	3.4481 00	1.4223 00	1.7458 00	1.0243 00	3.5080 00	10.0000-01
900.	1.6333 00	2.1649 00	3.5018 00	1.4281 00	1.8631 00	1.0327 00	3.5279 00	10.0000-01
1000.	1.7491 00	2.3306 00	3.5504 00	1.4347 00	1.9779 00	1.0427 00	3.5510 00	10.0000-01
1100.	1.8547 00	2.4825 00	3.5950 00	1.4424 00	2.0917 00	1.0545 00	3.5779 00	10.0000-01
1200.	1.9519 00	2.6231 00	3.6366 00	1.4517 00	2.2060 00	1.0683 00	3.6089 00	10.0000-01
1300.	2.0420 00	2.7544 00	3.6755 00	1.4629 00	2.3220 00	1.0841 00	3.6439 00	10.0000-01
1400.	2.1260 00	2.8778 00	3.7123 00	1.4765 00	2.4410 00	1.1023 00	3.6830 00	1.0000 00
1500.	2.2046 00	2.9945 00	3.7474 00	1.4927 00	2.5644 00	1.1232 00	3.7264 00	10.0000-01
1600.	2.2784 00	3.1052 00	3.7809 00	1.5116 00	2.6927 00	1.1465 00	3.7737 00	10.0000-01
1700.	2.3477 00	3.2108 00	3.8131 00	1.5335 00	2.8277 00	1.1729 00	3.8252 00	1.0000 01
1800.	2.4136 00	3.3117 00	3.8442 00	1.5582 00	2.9697 00	1.2024 00	3.8810 00	10.0000-01
1900.	2.4748 00	3.4085 00	3.8743 00	1.5853 00	3.1189 00	1.2350 00	3.9408 00	10.0000-01
2000.	2.5326 00	3.5013 00	3.9036 00	1.6149 00	3.2767 00	1.2713 00	4.0051 00	10.0000-01
2100.	2.5874 00	3.5907 00	3.9322 00	1.6480 00	3.4449 00	1.3113 00	4.0738 00	10.0000-01
2200.	2.6391 00	3.6768 00	3.9602 00	1.6840 00	3.6227 00	1.3546 00	4.1469 00	10.0000-01
2300.	2.6879 00	3.7599 00	3.9875 00	1.7207 00	3.8090 00	1.4019 00	4.2246 00	10.0000 01
2400.	2.7341 00	3.8402 00	4.0144 00	1.7583 00	4.0049 00	1.4534 00	4.3071 00	10.0000-01
2500.	2.7777 00	3.9179 00	4.0408 00	1.8000 00	4.2143 00	1.5093 00	4.3943 00	10.0000-01
2600.	2.8189 00	3.9930 00	4.0669 00	1.8460 00	4.4374 00	1.5689 00	4.4865 00	10.0000-01
2700.	2.8578 00	4.0657 00	4.0926 00	1.8912 00	4.6688 00	1.6324 00	4.5839 00	10.0000-01
2800.	2.8947 00	4.1363 00	4.1180 00	1.9348 00	4.9083 00	1.7006 00	4.6862 00	10.0000-01
2900.	2.9296 00	4.2047 00	4.1431 00	1.9791 00	5.1584 00	1.7736 00	4.7937 00	10.0000-01
3000.	2.9628 00	4.2711 00	4.1679 00	2.0241 00	5.4222 00	1.8515 00	4.9062 00	10.0000-01
3100.	2.9943 00	4.3355 00	4.1924 00	2.0703 00	5.6973 00	1.9341 00	5.0239 00	10.0000-01
3200.	3.0242 00	4.3981 00	4.2167 00	2.1174 00	5.9847 00	2.0215 00	5.1469 00	10.0000-01
3300.	3.0526 00	4.4589 00	4.2408 00	2.1660 00	6.2853 00	2.1136 00	5.2753 00	10.0000-01
3400.	3.0795 00	4.5180 00	4.2646 00	2.2166 00	6.5999 00	2.2103 00	5.4093 00	10.0000-01
3500.	3.1052 00	4.5755 00	4.2883 00	2.2688 00	6.9279 00	2.3114 00	5.5488 00	1.0000 00
3600.	3.1295 00	4.6315 00	4.3117 00	2.3230 00	7.2701 00	2.4169 00	5.6941 00	1.0000 00
3700.	3.1527 00	4.6859 00	4.3350 00	2.3802 00	7.6281 00	2.5267 00	5.8455 00	1.0000 00
3800.	3.1747 00	4.7389 00	4.3581 00	2.4399 00	8.0015 00	2.6406 00	6.0030 00	10.0000-01
3900.	3.1956 00	4.7905 00	4.3811 00	2.4710 00	8.3379 00	2.7587 00	6.1669 00	1.0000 00

Molecular Weight = 2.016

R = 1381 ft/°K

Z = $p/(g_p RT)$ $\gamma = (d \log p / d \log p)_s$ Z* = $\frac{\text{number of moles per mole}}{\text{at } 273.15^\circ\text{K, 1 atm}}$ 1 amagat = 1.744×10^{-4} lb-sec²/ft⁴

At T = 300°K, p = 44.6 psia,

 $\rho = 2.7615$ amagat,

a = 4343 ft/sec

TABLE III
HYDROGEN DATA FOR CHARACTERISTIC COMPUTATIONS

$T, ^\circ K$	\bar{T}	$\rho, \text{lb-sec}^2/\text{ft}^4$	$\bar{\rho}$	$p, \text{lb/ft}^2$	\bar{p}	$a, \text{ft/sec}$	\bar{a}
1.60000+03	1.00000+00	3.31102-02	1.00000+00	2.69624+06	1.00000+00	1.10961+04	1.00000+00
1.70000+03	1.06250+00	3.88384-02	1.17301+00	3.43842+06	1.27526+00	1.16524+04	1.05014+00
1.80000+03	1.12500+00	4.51400-02	1.36333+00	4.33769+06	1.60879+00	1.22375+04	1.10287+00
1.90000+03	1.18750+00	5.20189-02	1.57109+00	5.42074+06	2.01048+00	1.28524+04	1.15628+00
2.00000+03	1.25000+00	5.94513-02	1.79556+00	6.71210+06	2.48943+00	1.35026+04	1.21688+00
2.10000+03	1.31250+00	6.74468-02	2.03704+00	8.24829+06	3.05844+00	1.41957+04	1.27935+00
2.20000+03	1.37500+00	7.59734-02	2.29456+00	1.00545+07	3.72907+00	1.49284+04	1.34538+00
2.30000+03	1.43750+00	8.50083-02	2.56744+00	1.21747+07	4.51544+00	1.56961+04	1.41457+00
2.40000+03	1.50000+00	9.45500-02	2.85562+00	1.46473+07	5.43250+00	1.65034+04	1.48732+00
2.50000+03	1.56250+00	1.04535-01	3.15718+00	1.75170+07	6.49681+00	1.73663+04	1.56508+00
2.60000+03	1.62500+00	1.14937-01	3.47136+00	2.08237+07	7.72325+00	1.82856+04	1.64794+00
2.70000+03	1.68750+00	1.25708-01	3.79664+00	2.45183+07	9.13061+00	1.92392+04	1.73387+00
2.80000+03	1.75000+00	1.36855-01	4.13333+00	2.89640+07	1.07424+01	2.02261+04	1.82282+00
2.90000+03	1.81250+00	1.48307-01	4.47920+00	3.39046+07	1.25748+01	2.12609+04	1.91607+00
3.00000+03	1.87500+00	1.60089-01	4.83504+00	3.95056+07	1.46521+01	2.23438+04	2.01367+00
3.10000+03	1.93750+00	1.72132-01	5.19876+00	4.58204+07	1.69942+01	2.34774+04	2.11563+00
3.20000+03	2.00000+00	1.84400-01	5.56929+00	5.29247+07	1.96291+01	2.46618+04	2.22256+00
3.30000+03	2.06250+00	1.96862-01	5.94566+00	6.08778+07	2.25788+01	2.59005+04	2.33420+00
3.40000+03	2.12500+00	2.09441-01	6.32557+00	6.97523+07	2.58702+01	2.71969+04	2.45103+00
3.50000+03	2.18750+00	2.22209-01	6.71120+00	7.96267+07	2.95325+01	2.85485+04	2.57285+00
3.60000+03	2.25000+00	2.34997-01	7.09741+00	9.05855+07	3.35970+01	2.99586+04	2.69993+00
3.70000+03	2.31250+00	2.47891-01	7.48686+00	1.02674+08	3.80803+01	3.14339+04	2.83288+00
3.80000+03	2.37500+00	2.60772-01	7.87590+00	1.16000+08	4.30229+01	3.29726+04	2.97155+00
3.90000+03	2.43750+00	2.73629-01	8.26418+00	1.30635+08	4.84507+01	3.45588+04	3.09648+00

$T, ^\circ K$	$-\bar{x}_0$	\bar{t}_0	\bar{F}	$\bar{F} + \bar{a}$	M
1.60000+03	0.00000+00	0.00000+00	0.00000+00	1.00000+00	0.00000+00
1.70000+03	1.68631-01	5.80743-01	1.64926-01	1.21506+00	5.53017-01
1.80000+03	3.42805-01	8.27775-01	3.26531-01	1.42940+00	7.50564-01
1.90000+03	5.23695-01	1.02342+00	4.86704-01	1.64498+00	8.83570-01
2.00000+03	7.11885-01	1.19322+00	6.45178-01	1.86206+00	9.80553-01
2.10000+03	9.08269-01	1.34779+00	8.02538-01	2.08189+00	1.05350+00
2.20000+03	1.11305+00	1.49201+00	9.58591-01	2.30387+00	1.10893+00
2.30000+03	1.32897+00	1.62909+00	1.11362+00	2.52819+00	1.15166+00
2.40000+03	1.55063+00	1.76104+00	1.26779+00	2.75510+00	1.18404+00
2.50000+03	1.78473+00	1.88930+00	1.42120+00	2.98628+00	1.20716+00
2.60000+03	2.02944+00	2.01466+00	1.57354+00	3.22148+00	1.22254+00
2.70000+03	2.28552+00	2.13800+00	1.72500+00	3.45888+00	1.23308+00
2.80000+03	2.55432+00	2.26023+00	1.87616+00	3.69898+00	1.23997+00
2.90000+03	2.83570+00	2.38147+00	2.02670+00	3.94277+00	1.24289+00
3.00000+03	3.13065+00	2.50226+00	2.17683+00	4.19050+00	1.24264+00
3.10000+03	3.43935+00	2.62273+00	2.32636+00	4.44219+00	1.23957+00
3.20000+03	3.76296+00	2.74334+00	2.47556+00	4.69813+00	1.23431+00
3.30000+03	4.10173+00	2.86417+00	2.62427+00	4.95847+00	1.22704+00
3.40000+03	4.45645+00	2.98545+00	2.77255+00	5.22358+00	1.21804+00
3.50000+03	4.82797+00	3.10740+00	2.92047+00	5.49332+00	1.20777+00
3.60000+03	5.21723+00	3.23024+00	3.06814+00	5.76807+00	1.19642+00
3.70000+03	5.62378+00	3.35374+00	3.21513+00	6.04801+00	1.18386+00
3.80000+03	6.04927+00	3.47829+00	3.36173+00	6.33328+00	1.17053+00
3.90000+03	6.49437+00	3.60399+00	3.50856+00	6.60505+00	1.16390+00

$M = \bar{t}_0/\bar{a}$

$\bar{F} = \frac{1}{a_0} \int \frac{dp}{\rho a}$

Initial Conditions
 $(\bar{x} = 0, \bar{t} = 0)$:
 $T = 1600^\circ K$
 $p = 2.69624 \times 10^6 \text{ psf}$
 $= 18,720 \text{ psia}$
 $a = 11,096.1 \text{ ft/sec}$

TABLE IV
ISENTROPIC FLOW, REAL HYDROGEN

\bar{t}_o	\bar{t}''	At $\bar{x} = 0$					\bar{T}_p	\bar{P}_p
		\bar{a}	\bar{T}	\bar{p}	$\bar{\rho}$	$\bar{\rho}u$		
Isentropic, homogeneous flow								
0	0	1	1	1	1	0	1	1
0.581	0.746	1.050	1.062	1.275	1.17	0.68	1.13	1.6
0.828	1.154	1.103	1.125	1.609	1.36	1.126	1.25	2.5
1.023	1.510	1.158	1.187	2.010	1.57	1.606	1.35	3.5
1.231	1.914	1.231	1.265	2.615	1.88	2.315	1.47	5.1
1.629	2.743	1.415	1.437	4.515	2.567	4.18	1.77	11
2.138	3.863	1.734	1.687	9.131	3.797	8.11	2.18	28.7
2.623	4.949	2.116	1.937	16.99	5.199	13.64	(2.5)	(55)
3.107	6.027	2.573	2.187	29.53	6.711	20.86	--	--
3.604	7.113	3.096	2.437	48.45	8.264	29.8	--	--
Isentropic, nonhomogeneous flow ($M_{\bar{x}=0} = 1$)								
1.427	2.314	1.348	1.378	3.762	2.3	3.1	1.62	7.7
1.616	2.714	1.474	1.489	5.258	2.78	4.1	1.76	11
1.800	3.114	1.610	1.597	7.144	3.27	5.265	1.89	15.3
1.981	3.514	1.754	1.702	9.485	3.82	6.7	2.04	20.5
2.160	3.914	1.905	1.805	12.349	4.4	8.38	2.15	27.2
2.339	4.314	2.063	1.906	15.773	5	10.32	2.27	35
2.517	4.714	2.229	2.004	19.803	5.6	12.48	2.41	46
2.696	5.114	2.402	2.099	24.476	6.15	14.78	(2.55)	(60)
2.875	5.514	2.582	2.192	29.829	6.65	17.19	(2.67)	(75)
3.055	5.914	2.769	2.283	35.893	7.26	20.1	(2.79)	(100)

Values extrapolated beyond available thermodynamic data are shown in parentheses.

TABLE V
DEVIATIONS FROM EXACT LINEAR SCALING AS USED IN LAUNCH CYCLE
CALCULATIONS AND ACTUAL SHOTS

Caliber, in.	0.375	0.5	0.5	2.5
Calculation	✓	✓		✓
Launch			✓	
Normalized ⁽¹⁾ Projectile Mass	1	0.85	0.85	1
Normalized ⁽²⁾ $\frac{\text{Piston Mass}}{\text{Pump Tube Volume}}$	1	0.9	0.9	1
Normalized ⁽³⁾ Piston Velocity	1	1.1	1.15 - 1.09	1
Muzzle Velocity, kft/sec	29.18	31.7	30.1 - 29.7	30.45
Release Pressure*, kpsi	1.8	1.5	~1.5	1.8
Maximum Pump Tube Pressure, kpsi	405	600	----	383

*Bursting pressure of a diaphragm at the barrel entrance

(1) Given as ratio $\left(\frac{\text{projectile mass}}{\text{0.375-in. proj. mass}} \right) \left(\frac{0.375}{\text{caliber}} \right)^3$

(2) Ratioed to $\left[\frac{\text{(piston mass)}}{\text{(pump tube volume)}} \right]$
for the 0.375-in. caliber

(3) Ratioed to piston velocity in the 0.375-in.
caliber gun

DOCUMENT CONTROL DATA - R&D

(Security classification of title, body of abstract and indexing annotation must be entered when the overall report is classified)

1 ORIGINATING ACTIVITY (Corporate author) Arnold Engineering Development Center ARO, Inc., Contract Operator Arnold Air Force Station, Tennessee		2e REPORT SECURITY CLASSIFICATION UNCLASSIFIED	
		2b GROUP N/A	
3 REPORT TITLE CONSTANT ACCELERATION FLOWS AND APPLICATIONS TO HIGH-SPEED GUNS			
4 DESCRIPTIVE NOTES (Type of report and inclusive dates) N/A			
5 AUTHOR(S) (Last name, first name, initial) Lukasiewicz, J., ARO, Inc.			
6 REPORT DATE November 1966	7a TOTAL NO OF PAGES 51	7b NO OF REFS 7	
8a CONTRACT OR GRANT NO AF40(600)-1200	9a ORIGINATOR'S REPORT NUMBER(S) AEDC-TR-66-181		
b PROJECT NO	9b OTHER REPORT NO(S) (Any other numbers that may be assigned this report) N/A		
c Program Element 65402234			
d			
10 AVAILABILITY/LIMITATION NOTICES Distribution of this document is unlimited.			
11 SUPPLEMENTARY NOTES Available in DDC.		12 SPONSORING MILITARY ACTIVITY Arnold Engineering Development Center, Air Force Systems Command, Arnold Air Force Station, Tenn.	
13 ABSTRACT Solutions for isothermal, isentropic, and constant Mach number (at a specified location) flows with constant acceleration are obtained. It is shown that in application to high-speed guns, these solutions necessitate variable gun geometry or heating of the propellant; both requirements are considered at present impractical. Numerical solutions which give constant projectile acceleration in a fixed geometry gun are computed for ideal and real hydrogen propellant. Using the latter, and the appropriate similarity parameters, as well as practical constraints related to gun and projectile geometry and strength, it is shown that a substantial increase in muzzle velocity could be obtained if the constant base pressure cycle were more closely approximated in actual launchings. At present the velocity attained with large caliber guns is much smaller than with the small ones. In this connection, the validity of linear scaling of guns and the resulting possibility of application of small-scale developments to large caliber guns are indicated.			

14. KEY WORDS	LINK A		LINK B		LINK C	
	ROLE	WT	ROLE	WT	ROLE	WT
high-speed guns constant acceleration flows solutions variable gun geometry 3 fixed geometry gun 5 hydrogen propellants 6 muzzle velocity 7 linear scaling 8 light-gas launchers 9 launchers						

2. Guns
 4 Hydrogen

INSTRUCTIONS

1. **ORIGINATING ACTIVITY:** Enter the name and address of the contractor, subcontractor, grantee, Department of Defense activity or other organization (*corporate author*) issuing the report.
- 2a. **REPORT SECURITY CLASSIFICATION:** Enter the overall security classification of the report. Indicate whether "Restricted Data" is included. Marking is to be in accordance with appropriate security regulations.
- 2b. **GROUP:** Automatic downgrading is specified in DoD Directive 5200.10 and Armed Forces Industrial Manual. Enter the group number. Also, when applicable, show that optional markings have been used for Group 3 and Group 4 as authorized.
3. **REPORT TITLE:** Enter the complete report title in all capital letters. Titles in all cases should be unclassified. If a meaningful title cannot be selected without classification, show title classification in all capitals in parenthesis immediately following the title.
4. **DESCRIPTIVE NOTES:** If appropriate, enter the type of report, e.g., interim, progress, summary, annual, or final. Give the inclusive dates when a specific reporting period is covered.
5. **AUTHOR(S):** Enter the name(s) of author(s) as shown on or in the report. Enter last name, first name, middle initial. If military, show rank and branch of service. The name of the principal author is an absolute minimum requirement.
6. **REPORT DATE:** Enter the date of the report as day, month, year, or month, year. If more than one date appears on the report, use date of publication.
- 7a. **TOTAL NUMBER OF PAGES:** The total page count should follow normal pagination procedures, i.e., enter the number of pages containing information.
- 7b. **NUMBER OF REFERENCES:** Enter the total number of references cited in the report.
- 8a. **CONTRACT OR GRANT NUMBER:** If appropriate, enter the applicable number of the contract or grant under which the report was written.
- 8b, 8c, & 8d. **PROJECT NUMBER:** Enter the appropriate military department identification, such as project number, subproject number, system numbers, task number, etc.
- 9a. **ORIGINATOR'S REPORT NUMBER(S):** Enter the official report number by which the document will be identified and controlled by the originating activity. This number must be unique to this report.
- 9b. **OTHER REPORT NUMBER(S):** If the report has been assigned any other report numbers (either by the originator or by the sponsor), also enter this number(s).
10. **AVAILABILITY/LIMITATION NOTICES:** Enter any limitations on further dissemination of the report, other than those

imposed by security classification, using standard statements such as:

- (1) "Qualified requesters may obtain copies of this report from DDC."
- (2) "Foreign announcement and dissemination of this report by DDC is not authorized."
- (3) "U. S. Government agencies may obtain copies of this report directly from DDC. Other qualified DDC users shall request through _____."
- (4) "U. S. military agencies may obtain copies of this report directly from DDC. Other qualified users shall request through _____."
- (5) "All distribution of this report is controlled. Qualified DDC users shall request through _____."

If the report has been furnished to the Office of Technical Services, Department of Commerce, for sale to the public, indicate this fact and enter the price, if known.

11. **SUPPLEMENTARY NOTES:** Use for additional explanatory notes.
12. **SPONSORING MILITARY ACTIVITY:** Enter the name of the departmental project office or laboratory sponsoring (paying for) the research and development. Include address.
13. **ABSTRACT:** Enter an abstract giving a brief and factual summary of the document indicative of the report, even though it may also appear elsewhere in the body of the technical report. If additional space is required, a continuation sheet shall be attached.

It is highly desirable that the abstract of classified reports be unclassified. Each paragraph of the abstract shall end with an indication of the military security classification of the information in the paragraph, represented as (TS), (S), (C), or (U)

There is no limitation on the length of the abstract. However, the suggested length is from 150 to 225 words.

14. **KEY WORDS:** Key words are technically meaningful terms or short phrases that characterize a report and may be used as index entries for cataloging the report. Key words must be selected so that no security classification is required. Identifiers, such as equipment model designation, trade name, military project code name, geographic location, may be used as key words but will be followed by an indication of technical context. The assignment of links, rules, and weights is optional.